HOKKAIDO UNIVERSITY

Title	Activation of invariant natural killer T cells by alpha-galactosylceramide ameliorates myocardial ischemia/reperfusion injury in mice
Author(s)	Homma, Tsuneaki; Kinugawa, Shintaro; Takahashi, Masashige et al.
Citation	Journal of molecular and cellular cardiology, 62, 179-188 https://doi.org/10.1016/j.yjmcc.2013.06.004
Issue Date	2013-09
Doc URL	https://hdl.handle.net/2115/53280
Type	journal article
File Information	JMCC7413 R1.pdf

Hokkaido University Collection of Scholarly and Academic Papers : HUSCAP

Activation of Invariant Natural Killer T Cells by α-galactosylceramide Ameliorates Myocardial Ischemia/Reperfusion Injury in Mice

Tsuneaki Homma, MD; Shintaro Kinugawa, MD, PhD; Masashige Takahashi, MD, PhD; Mochamad Ali Sobirin, MD, PhD; Akimichi Saito, MD; Arata Fukushima, MD; Tadashi Suga, PhD; Shingo Takada, BS; Tomoyasu Kadoguchi, BS; Yoshihiro Masaki, MD; Takaaki Furihata, MD; Masaru Taniguchi, MD, PhD; Toshinori Nakayama, MD, PhD; Naoki Ishimori, MD, PhD; Kazuya Iwabuchi, MD, PhD; and Hiroyuki Tsutsui, MD, PhD

Department of Cardiovascular Medicine, Hokkaido University Graduate School of Medicine, Sapporo, Japan (T.H., S.K., M.T., M.A.S., A.S., A.F., T.S., S.T.,T.K., Y.M., T.F., N.I., H.T.); Faculty of Medicine, Diponegoro University, Semarang, Indonesia (M.A.S); RIKEN Research Center for Allergy and Immunology, Kanagawa, Japan (M.T.); Department of Immunology, Graduate School of Medicine, Chiba University, Chiba, Japan (T.N.); Department of Immunology, Kitasato University School of Medicine, Sagamihara, Japan (K.I.).

Corresponding author: Shintaro Kinugawa, MD, PhD

Address: Department of Cardiovascular Medicine, Hokkaido University Graduate School of Medicine, Kita-15, Nishi-7, Kita-ku, Sapporo 060-8638, Japan

Tel number: +81-11-706-6973

Fax number: +81-11-706-7874

E-mail address: tuckahoe@med.hokudai.ac.jp

The number of words: 6856 words

Abstract

Invariant natural killer T (iNKT) cells orchestrate tissue inflammation via regulating various cytokine productions. However the role of iNKT cells has not been determined in myocardial ischemia/reperfusion (I/R) injury. The purpose of this study was to examine whether the activation of iNKT cells by α-galactosylceramide (α-GC), which specifically activates iNKT cells, could affect myocardial I/R injury. I/R or sham operation was performed in male C57BL/6J mice. I/R mice received the injection of either αGC (I/R+αGC, n=48) or vehicle (I/R+vehicle, n=49) 30 min before reperfusion. After 24 hr, infarct size/area at risk was smaller in I/R+αGC than in I/R+vehicle (37.8±2.7% vs 47.1±2.5%, $P<0.05$), with no significant changes in area at risk. The numbers of infiltrating myeloperoxidase- and CD3-positive cells were lower in I/R+αGC. Apoptosis evaluated by TUNEL staining and caspase-3 protein was also attenuated in I/R+αGC. Myocardial gene expression of tumor necrosis factor-α and interleukin (IL)-1β in I/R+αGC was lower to 46% and 80% of that in I/R+vehicle, respectively, whereas IL-10, IL-4, and interferon (IFN)-γ were higher in I/R+αGC than I/R+vehicle by 2.0, 4.1, and 9.6 folds, respectively. The administration of anti-IL-10 receptor antibody into I/R+αGC abolished the protective effects of αGC on I/R injury (infarct size/area at risk: 53.1±5.2% vs 37.4±3.5%, $P<0.05$). In contrast, anti-IL-4 and anti-IFN-γ antibodies did not exert such effects. In conclusion, activated iNKT cells by αGC play a protective role against myocardial I/R injury through the enhanced expression of IL-10. Therapies designed to activate iNKT cells might be beneficial to protect the heart from I/R injury.

Highlights

• α-galactosylceramide rapidly increases gene expression of cytokines in the heart.

• α-galactosylceramide ameliorates myocardial ischemia/reperfusion injury.

• IL-10 was involved in the protective effects of αGC in myocardial I/R injury.

Key words

invariant natural killer T cells, myocardial ischemia/reperfusion injury, inflammation, cytokines.

Abbreviations	
AAR	area at risk
αGC	α-galactosylceramide
IFN-γ	interferon-γ
IL	interleukin
iNKT	invariant natural killer T
I/R	ischemia/reperfusion
IS	infarct size
LV	left ventricle
MI	myocardial infarction
MNCs	mononuclear cells
MPO	myeloperoxidase
NK	natural killer
qRT-PCR	quantitative reverse transcriptase-polymerase chain reaction
TCR	T cell receptor
T_H1	T-helper type 1
T_H2	T-helper type 2
TGF-β	transforming growth factor-β

TNF-α	tumor necrosis factor-α
TTC	2,3,5-triphenyltetrazolium chloride

1. Introduction

Early and successful myocardial reperfusion is the most effective strategy to reduce infarct size and preserve cardiac function after acute myocardial infarction (MI) [1]. Reperfusion after ischemia can salvage the ischemic myocardium, however, simultaneously it causes additional cell death and attenuates the beneficial effects of reperfusion itself, called myocardial ischemia/reperfusion (I/R) injury [2]. Inflammation has been shown to play a critical role in the pathophysiology of myocardial I/R injury [3], and various immune cells, such as neutrophils, T lymphocytes, monocytes/macrophages, and mast cells, are involved in myocardial I/R injury [4-7]. Recent study by Yang et al demonstrated that $CD4^+$ T lymphocytes played an important role in the development of I/R injury and interferon (IFN)-γ was involved in their action by using Rag1 knockout mice lacking mature lymphocytes [5].

Invariant natural killer T (iNKT or type 1 NKT) cells are innate-like T lymphocyte population characterized by co-expressing NK lineage receptors and T cell receptors (TCR), and their TCR has invariant α-chain (Vα14-Jα18 in mice, and Vα24-Jα18 in humans) [8, 9]. They are activated by recognizing glycolipid antigens presented by CD1d, a member of major histocompatibility complex (MHC) class I like molecules, and rapidly secrete a mixture of large amount of T-helper type 1 (T_H1) and T_H2 cytokines, such as IFN-γ, interleukin (IL)-10 and IL-4 in shaping subsequent adaptive immune responses [10]. Thus, iNKT cells can function as a bridge between the innate and adaptive immune systems, and orchestrate tissue inflammation.

iNKT cells have been demonstrated to play a protective role in various autoimmune and inflammatory diseases such as type 1 diabetes, experimental allergic encephalomyelitis, rheumatoid arthritis, and enteritis [11-15]. We have also reported that the activation of iNKT cells by α-galactosylceramide (αGC), a specific activator for iNKT cells [16], can attenuate the development of left ventricular (LV) remodeling and failure after MI created by chronic ligation of coronary artery in mice [17]. The activation of iNKT cells by αGC has been also reported to protect the liver against I/R injury in mice via IL-13 production [18]. However, no previous studies have examined the effects of iNKT cell activation by αGC on myocardial I/R injury.

Therefore, the purpose of the present study was to determine whether the activation of iNKT cells by αGC could attenuate myocardial I/R injury. We also determined whether the protective effects on attenuated myocardial I/R injury might involve the activation of anti-inflammatory cytokines including IL-10.

2. Materials and Methods

Detailed methods are available in the Online Supplementary Material.

2.1 Animals

C57BL/6J mice were purchased from CLEA Japan, Inc. (Tokyo, Japan). Animals were used for experiments at 10 to 12 weeks of age (weight 23-27 g). Mice were bred in a pathogen-free environment and kept under a constant 12-h light–dark cycle at a temperature of 23°C to 25°C. Standard chaw and water were provided.

All procedures and animal care were approved by our institutional animal research committee and conformed to the animal care guideline for the Care and Use of Laboratory Animals in Hokkaido University Graduate School of Medicine.

2.2 Experimental Design

Experiment 1: Effects of αGC on iNKT Cell and Cytokine Expression in the Normal Mice

To confirm that αGC could activate iNKT cells in the heart similar to the spleen, C57BL/6J mice were sacrificed 0, 24, and 72 hr after αGC (Funakoshi Co., Ltd., Tokyo, Japan) injection (0.1 μg/g body weight i.p., n=9 for each group) and the proportion of iNKT cells in the heart and spleen were measured by flow cytometric analysis [17].

To determine that αGC could induce the changes of cytokines in the blood and the heart within 24

hr, another group of C57BL/6J mice were sacrificed 0, 0.5, 1, 3, 6, 12, and 24 hr after single injection of αGC (n=6 for each group). Serum levels of IL-10, IL-4, and IFN-γ were measured by ELISA and their gene expressions in the heart were measured by quantitative reverse transcriptase-polymerase chain reaction (qRT-PCR). TCR in iNKT cells has invariant α-chain encoded by Vα14-Jα18 gene segment in mice, and $J\alpha18^{-/-}$ mice lack iNKT cells. To confirm whether the changes of cytokines by the injection of αGC were due to the activation of iNKT cells, iNKT cell-deficient ($J\alpha18^{-/-}$) mice were sacrificed after single injection of αGC and same measurements were performed. They were provided from Dr. M. Taniguchi (RIKEN, Yokohama, Japan) and backcrossed 10 times to C57BL/6J.

Experiment 2: Effects of αGC on Myocardial I/R Injury

Myocardial I/R surgery or sham operation was performed in C57BL/6J mice according to the methods described previously [5]. After anesthesia, the left coronary artery was ligated for 45 min. Ischemia was confirmed by bleaching of the myocardium. Reperfusion was initiated by releasing the ligature. Sham-operated mice underwent a similar procedure without ligation. αGC (0.1 μg/g body weight i.p.) was administered 30 min before reperfusion to specifically activate iNKT cells. As control, the same volume of vehicle was administered into sham and I/R mice.

Mice were sacrificed 24 hr after reperfusion (Sham+vehicle, n=22; Sham+αGC, n=22; I/R+vehicle, n=49, I/R+αGC, n=48). These mice were divided into groups for some measurements. Another groups of mice were sacrificed 72 hr after reperfusion for flow cytometric analysis (n=9 for each group), because iNKT cells have been reported to be invisible by flow-cytometric detection 24 hr after αGC

administration [19]. Additional mice were sacrificed 72 hr after reperfusion for RT-PCR analysis (n=7-8 for each group). To confirm early protective effect of αGC, C57BL/6J mice were received I/R surgery with vehicle or αGC, and sacrificed 2 hr after reperfusion to measure infarct size (I/R+vehicle, n=7; I/R+αGC, n=8). Furthermore, to confirm the effect of αGC-induced reduction of infarct size on long-term LV function and remodeling, echocardiography and hemodynamic measurement were performed at 28 days after reperfusion (I/R+vehicle, n=8; I/R+αGC, n=8).

To confirm whether the effect of αGC on infarct size in I/R was due to the activation of iNKT cells, Jα18$^{-/-}$ mice were received I/R surgery with vehicle or αGC and sacrificed 24 hr after reperfusion to measure infarct size (n=5 for each group).

Furthermore, to examine the role of various cytokines in the effects of αGC on myocardial I/R injury, rat anti-IL-10 receptor monoclonal antibody (200μg/mouse, i.p., BD Pharmingen, San Diego, CA), rat anti-IL-4 monoclonal antibody (250μg/mouse, i.p., R&D System, Inc.), or rat anti-IFN-γ monoclonal antibody (150μg/mouse, i.p., R&D System, Inc.) was administered 90 min before I/R surgery and infarct size was measured 24 hr after reperfusion. The doses of these antibodies were chosen based on the previous study of their efficacy [18, 20, 21]. We also confirmed that the changes of serum IL-4 or IFN-γ levels were completely inhibited by identical antibodies. Rat IgG1κ was used as control. αGC was administered 30 min before reperfusion (I/R+αGC+rat IgG1κ, n=8; I/R+αGC+anti-IL-10R, n=8; I/R+αGC+anti-IL-4, n=7; I/R+αGC+anti-IFN-γ, n=9).

Finally, to examine the role of IFN-γ on myocardial I/R injury, rat anti-IFN-γ monoclonal antibody

(150μg/mouse, i.p., R&D System, Inc.) or IgG1κ was administered 90 min before I/R surgery and infarct size was measured 24 hr after reperfusion (n=6 for each).

2.3 Statistical Analysis

Data are expressed as means±SE. The Student *t* test was performed for comparison between 2 independent groups. For multiple-group comparisons, one-way ANOVA followed by the Dunnett's test or the Tukey's test was performed. A value of $P<0.05$ was considered statistically significant.

The authors had full access to and take full responsibility for the integrity of the data. All authors had read and agree to the manuscript as written.

3. Results

Experiment 1: Effects of αGC on iNKT Cell and Cytokine Expression in the Normal Mice

3.1 Proportion of iNKT Cells after αGC Administration

After αGC administration, splenic iNKT cells disappeared at 24 hr and were increased at 72 hr (**Supplemental Figure 1, upper panel**) in consistency with the previous report [19]. The number of cardiac iNKT cells itself was lower than that of splenic iNKT cells. However, they were increased 72 hr after αGC administration in parallel to splenic iNKT cells (**Supplemental Figure 1, lower panel**). Similar results were observed in 3 independent experiments.

3.2 Serum Levels and Myocardial Gene Expression of Cytokines after αGC Administration

After the administration of αGC, serum IL-10 and IL-4 levels were rapidly increased and peaked at 1 hr and 3 hr respectively, and serum IFN-γ levels were increased later and peaked at 12 hr (**Supplemental Figure 2A**), which was consistent with the previous reports [22, 23]. Gene expression of IL-10, IL-4, and IFN-γ in the LV was increased within 24 hr and peaked at later phase than serum levels (**Supplemental Figure 2B**).

3.3 Specificity of αGC for iNKT cells

αGC did not increase serum levels and myocardial gene expression of IL-10, IL-4, and IFN-γ in

Jα18$^{-/-}$ mice (**Figure 1**).

Experiment 2: Effects of αGC on Myocardial I/R Injury

3.4 Body weight and hemodynamics

There was no difference in body weight among all groups. Systolic blood pressure was significantly lower in I/R mice compared to sham mice, however, which was not affected by αGC. Diastolic blood pressure and heart rate did not differ among 4 groups.

3.5 iNKT cells

Representative flow cytometric analyses from 4 groups of mice are shown in **Figure 2A**. The proportion of iNKT cells 72 hr after reperfusion was increased up to 2.7-fold in I/R+vehicle compared to Sham+vehicle. αGC significantly increased these proportion of iNKT cells both in sham up to 17.5-fold (P=0.042) and I/R mice up to 10.3-fold (P=0.004) (**Figure 2B**). Similar results were observed in 3 independent experiments.

3.6 I/R Injury and LV function

The administration of αGC into I/R mice decreased infarct size. IS/AAR was significantly smaller in I/R+αGC than in I/R+vehicle (37.8±2.7% vs 47.1±2.5%, P=0.018) without significant changes in

AAR/LV (58.5±2.3% vs 58.9±2.7%, *P*=NS) at 24 hr after reperfusion (**Figure 3A**). In consistent with these results, serum level of troponin-I was also lower in I/R+αGC than in I/R+vehicle (5.8±0.8 ng/mL vs 8.7±0.7ng/mL, *P*=0.016, **Figure 3B**). At 2 hr after reperfusion, IS/AAR was also smaller in I/R+αGC than in I/R+vehicle (20.7±1.8% vs 29.9±2.8%, *P*=0.014) without significant changes in AAR/LV (**Supplemental Figure 3**). To examine whether the reduction in infarct size by αGC was due to the activation of iNKT cells, Jα18$^{-/-}$ mice were used. There were no differences in IS/AAR between Jα18$^{-/-}$+I/R+αGC and Jα18$^{-/-}$+I/R+vehicle (34.9±4.7% vs 35.6±4.1%, *P*=NS) and in AAR/LV between groups (51.3±6.4% vs 59.0±2.4%, *P*=NS) at 24 hr after reperfusion (**Supplemental Figure 4**).

Echocardiography and hemodynamic data at 28 days after reperfusion were shown in **Table 1**. LV end-diastolic dimension did not differ between 2 groups, whereas LV end-systolic dimension was significantly decreased in I/R+αGC compared to I/R+vehicle, which resulted in greater fractional shortening in I/R+αGC. Furthermore, anterior wall thickness including infarct region was preserved in I/R+αGC. There were no differences in HR, BP, and LV ±dP/dt between groups. LV end-diastolic pressure was decreased in I/R+αGC.

3.7 Inflammatory Cell Infiltration

Immunohistochemical analysis revealed that the number of MPO (as a marker of neutrophil)- and CD3 (as a marker of T lymphocyte)-positive cells and the ratio of MAC3 (as a marker of

macrophage)-positive area in the ischemic myocardium were increased in I/R+vehicle compared to Sham+vehicle. Administration of αGC into I/R mice significantly ameliorated the infiltration of MPO- and CD3-positive cells in I/R mice. In contrast, there were no significant differences in MAC3-positive area between I/R+vehicle and I/R+αGC (**Figure 4A, B**).

Flow cytometric analysis also showed that $CD45^+$ cells (leukocytes), $CD45^+Ly6G^+$ cells (neutrophils), and Ly6Chigh monocytes in the ischemic heart were decreased in I/R+αGG compared to I/R+vehicle (**Supplemental Figure 5**). In contrast, $CD45^+CD68^+$ cells excluding monocytes (macrophages) were comparable between groups (**Supplemental Figure 5**).

3.8 TUNEL Staining and Caspase-3 Protein

There were rare TUNEL-positive nuclei both in Sham+vehicle and Sham+αGC mice. There were some cardiomyocytes with TUNEL-positive nuclei in I/R+vehicle and I/R+αGC (**Figure 5A**). The number of TUNEL-positive cardiomyocytes in the ischemic LV was increased in I/R+vehicle compared to Sham+vehicle. It was significantly decreased in I/R+αGC compared to I/R+vehicle (**Figure 5B**). Full length caspase-3 protein levels were significantly increased in the ischemic myocardium from I/R+vehicle compared to Sham+vehicle, which was consistent with previous papers [24, 25], and this increase was also inhibited in I/R+αGC (**Figure 5C**).

3.9 Serum and Myocardial Cytokines, and Chemokines

Very small amounts of serum IL-10 and IFN-γ levels were detected and IL-4 was not detected in either Sham+vehicle or I/R+vehicle mice. In contrast, αGC extremely increased these cytokine levels in both sham and I/R mice (**Figure 6A**). At 24 hr after reperfusion, gene expression of IL-10, IL-4, and IFN-γ in the ischemic myocardium tended to be increased in I/R+vehicle compared to Sham+vehicle, and they were significantly increased in I/R+αGC compared to I/R+vehicle (**Figure 6B**). These gene expressions were also measured at 72 hr after reperfusion in another set of mice. Gene expression of IL-10 was significantly increased in both I/R+vehicle and I/R+αGC, and tended to be increased by αGC in sham and I/R (**Supplemental Figure 6A**). IL-4 and IFN-γ were increased in I/R+αGC compared to I/R+vehicle (**Supplemental Figure 6B, C**).

Gene expression of TNF-α, IL-1β, and TGF-β1 was significantly increased in I/R+vehicle compared to Sham+vehicle. In contrast to IL-10, IL-4, and IFN-γ, TNF-α, and IL-1β were lower in I/R+αGC than I/R+vehicle (**Figure 6B**). MCP-1, ICAM-1, and VCAM-1 were increased in I/R+vehicle (**Supplemental Figure 7**). MCP-1 was decreased in I/R+αGC compared to I/R+vehicle (**Supplemental Figure 7**), which could inhibit infiltration of inflammatory cells (**Figure 4 and Supplemental Figure 5**). In contrast, there was no difference in ICAM-1, and VCAM-1 was rather increased in I/R+αGC compared to I/R+vehicle (**Supplemental Figure 7**).

3.10 Effects of Neutralization of IL-10, IL-4, and IFN-γ on αGC-Treated I/R Mice.

Representative pictures showed that the administration of anti-IL-10 receptor monoclonal antibody

into I/R+αGC mice increased infarct size compared to I/R+αGC+rat IgG1κ. In contrast, the administration of anti-IL-4 and anti-IFN-γ did not affect it (**Figure 7, upper panels**). IS/AAR was significantly greater in I/R+αGC+anti-IL-10R than I/R+αGC+rat IgG1κ (53.1±5.2% vs 37.4±3.5%, *P*=0.046) with no significant changes in AAR/LV (54.3±2.0% vs 54.7±2.9%, *P*=NS) (**Figure 7, lower panel**).

3.11 Effects of Neutralization of IFN-γ on I/R mice

Representative pictures showed that the administration of anti-IFN-γ monoclonal antibody into I/R mice decreased infarct size compared to I/R+rat IgG1κ (**Supplemental Figure 8, upper panels**). IS/AAR was significantly smaller in I/R+ anti-IFN-γ than I/R+rat IgG1κ (38.0±3.7% vs 49.7±1.9%, *P*=0.020) with no significant changes in AAR/LV (56.4±4.1% vs 57.8±1.5%, *P*=NS) (**Supplemental Figure 8, lower panel**).

4. Discussion

The present study demonstrated that the activation of iNKT cells by αGC ameliorated myocardial I/R injury, accompanied by the decreases in inflammatory cell infiltration, apoptosis, and pro-inflammatory cytokines. Furthermore, the neutralization of αGC-induced increase in expression of IL-10 by receptor antibody abolished the protective effects of αGC on I/R injury. This is the first report to provide direct evidence for the protective effects of iNKT cell activation by αGC on myocardial I/R injury.

4.1 Activation of iNKT Cells by αGC in the Heart

αGC has been well known to activate iNKT cells, and they rapidly produce various cytokines such as IL-10, IL-4, and IFN-γ [26]. In parallel to these changes, iNKT cell-surface receptors, including TCR and NK1.1, become donwregulated, which render iNKT cells invisible by flow-cytometric detection [19, 27]. The downregulation of TCR remains until at least 24 hr. Then, iNKT cells rapidly proliferate and increase to the peak level 72 hr after αGC administration. The activation of iNKT cells by αGC has been observed in various organs, such as spleen, liver, lung, and kidney [18, 19, 27-29]. We previously demonstrated that the proportion of iNKT cells was increased within the heart 7 day after αGC administration [17]. In the present study, we confirmed that αGC increased cardiac iNKT cells in parallel to splenic iNKT cells (**Supplemental Figure 1**) and rapidly enhanced the expression

of cytokine genes within the heart (**Supplemental Figure 2B**), however, αGC had no effect in iNKT cell-deficient (Jα18$^{-/-}$) mice (**Figure 1**). Therefore, these findings indicate that αGC can specifically activate iNKT cells, which results in the production of cytokines in the heart.

4.2 Myocardial I/R Injury and Cytokines

It is well known that various cytokines are involved in myocardial I/R injury [30, 31]. These cytokines are produced by several types of cells, such as neutrophils, lymphocytes, macrophages, and endothelial cells, and play an important role in the pathogenesis of myocardial I/R injury. Endogenous TNF-α and IL-1 play as a mediator of inflammatory reactions, whereas, IL-10 and TGF-β have cardioprotective effects on myocardial I/R injury. Previous studies demonstrated that the blocking of pro-inflammatory cytokines or the administration of cardioprotective cytokines reduced infarct size [32-37]. On the other hand, the increases in IL-4 and IFN-γ are characteristic of the activation of iNKT cells [9]. IFN-γ has been reported to promote myocardial I/R injury [5], and the effect of IL-4 on myocardial I/R injury has not been elucidated. In the present study, αGC administration decreased infarct size (**Figure 3**) and infiltrating inflammatory cells (**Figure 4 and Supplemental Figure 5**) in association with the decrease in the expressions of pro-inflammatory cytokines, TNF-α and IL-1β (**Figure 6B**). Simultaneously, serum levels and gene expression of IL-10, IL-4, and IFN-γ were increased after αGC administration (**Figure 6A, B**).

To determine the role of these cytokines in αGC-induced amelioration of myocardial I/R injury, we

neutralized IL-10, IL-4, and IFN-γ on αGC-treated I/R mice. Anti-IL-10R monoclonal antibody canceled the protective effects of αGC in I/R mice, but not anti-IL-4 and IFN-γ monoclonal antibody (**Figure 7**), indicating that IL-10 was involved in the protective effects of αGC in myocardial I/R injury. Yang et al reported that INF-γ had deleterious effects on myocardial I/R injury [5]. We also showed that a single treatment with anti-IFN-γ monoclonal antibody reduced infarct size after I/R injury without αGC (**Supplemental Figure 8**). In our results, the reduction in infarct size by αGC was the same as that by anti-IFN-γ monoclonal antibody, and there was no additional reduction in infarct size by αGC and anti-IFN-γ monoclonal antibody. These results suggested that IL-10-dependent beneficial effects of αGC may be due to the inhibition of INF-γ-dependent deleterious effects on myocardial I/R injury. Indeed, it has been reported that IL-10 inhibits the expression of IFN-γ-induced genes [38].

We showed that infarct size was smaller in I/R+αGC than I/R+vehicle also at 2 hr after reperfusion (**Supplemental Figure 3**). Serum IL-10 was rapidly increased and peaked at 1 hr after αGC injection, in contrast, gene expression of IL-10 in the LV was not increased at early phase after αGC injection (**Supplemental Figure 2**). Therefore, the improvement in infarct size by αGC may be due to the increased serum IL-10, i.e. systemic activation of iNKT cells.

4.3 Protective Effects of IL-10 on Myocardial I/R Injury

IL-10 is well known as a potent anti-inflammatory cytokine [39], and has been shown to play an

important role in myocardial I/R injury [34]. It has been reported that endogenous IL-10 inhibits the production of TNF-α and serves to protect the reperfused myocardium through the suppression of neutrophil recruitment [34]. IL-10 has been reported to suppress the expression of CC chemokine gene including MCP-1 [40]. Exogenous IL-10 administration ameliorates myocardial I/R injury by inhibiting adherence of leukocytes to vascular endothelium [35], and by decreasing the production of pro-inflammatory cytokines through Signal Transducers and Activator of Transcription (STAT)-3 pathway [36]. It has also been shown that remote ischemic preconditioning has protective effects against myocardial I/R injury by the upregulation of IL-10 in the remote muscle and the release into circulation [41]. Moreover, IL-10 induces protection against myocardial injury by preventing apoptosis through the reduced phosphorylation of p38MAPK and the enhanced phosphorylation of STAT3 [42]. TNF-α and IL-1β promotes apoptosis in cardiac myocytes [43, 44], which is also inhibited by IL-10. In the present study, we demonstrated that αGC administration ameliorated myocardial I/R injury (**Figure 3**) with upregulating serum and myocardial IL-10 (**Figure 6**). This was accompanied with the decreases in the infiltration of inflammatory cells into myocardium (**Figure 4 and Supplemental Figure 5**) and the gene expression of pro-inflammatory cytokines (**Figure 6B**), and the reduction in apoptosis after I/R (**Figure 5**). Our results suggest that the activated iNKT cells by αGC inhibit inflammatory response and cardiomyocyte apoptosis via the production of IL-10.

We previously demonstrated that administration of αGC into mice 1 day and 4 day after MI surgery ameliorated LV remodeling without affecting infarct size and these beneficial effects were

also mediated by the enhanced expression of IL-10 in the heart [17]. On the other hand, in the present study, we demonstrated that αGC administration decreased infarct size. The discrepancy in the effects of αGC on infarct size was possibly due to the differences in experimental model assessing different pathophysiological processes (more angiogenesis, more fibrosis vs. accentuated inflammation and apoptosis in the acute setting) and the timing of αGC treatment (1 day after MI surgery vs. 30 min before reperfusion). The administration of αGC into MI mice was performed too late to salvage ischemic myocardium.

4.4 Clinical Implication

The present study demonstrated that αGC administration during the ischemic period before reperfusion reduced infarct size. These findings suggest that αGC can be a novel agent in patients with acute MI to reduce I/R injury. In addition, based on our previous study of postinfarct heart failure [17], αGC administration may attenuate also LV remodeling and reduce mortality after MI. To date, several clinical trials (Phase I/II) using activated iNKT cells by αGC have been conducted in patients with cancer [45-49]. No severe adverse events were observed in these trials.

4.5 Limitations

There are several limitations to be acknowledged in the present study. First, we could not directly demonstrate the activation of iNKT cells within the heart 24 hr after αGC administration because

cell-surface receptors were downregulated. We tried double immunohistochemical staining of anti-TCRβ and anti-NK1.1 accoring to the newly published paper [50]. Furthermore, we also performed in situ hybridization using digoxigenin-labeled DNA probes for mouse Vα14Jα18. Unfortunately, however, we could not detect iNKT cells by these methods in the heart. Further studies are needed to overcome some technical difficulties of iNKT cell-detection and clarify this important issue. Alternatively, we demonstrated its activation by showing the increase of cytokine gene expressions and the similar time course of iNKT cell proportion within the spleen. Second, the source of IL-10 production after the stimulation of αGC remains to be determined. We tried to isolate iNKT cells using cell sorter and perform *in vitro* experiments. Unfortunately, however, we could not isolate sufficient amount of iNKT cells to perform *in vitro* experiments. We consider that there still might be some technical difficulties in *in vitro* experiments using isolated iNKT cells. Therefore, we could not directly demonstrate the source of IL-10 production. IL-10 has been shown to be produced by iNKT cells themselves on exogenous stimulation [51]. However, αGC-activated iNKT cells may stimulate other immune cells to produce IL-10. IL-10 can be also expressed and secreted from macrophages activated by iNKT cells. Moreover, in myocardial I/R injury, it has reported that CD5 positive T lymphocytes are the predominant source of IL-10 in the ischemic and reperfused heart. However, immunohistochemical analysis and flow cytometric analysis revealed that there was no difference in the infiltration of macrophage in the ischemic myocardium between from I/R+αGC and I/R+vehicle, and other inflammatory cells were rather decreased in I/R+αGC compared to I/R+vehicle (**Figure 4**

and Supplemental Figure 5). Further investigations are required to elucidate the mechanism of IL-10 production after αGC administration in I/R mice. Third, we observed that iNKT cells were increased and endogenously activated in ischemic myocardium after I/R, however, the clear evidence on the role of iNKT cells in I/R injury has not been shown in the present study. We performed I/R injury experiment using iNKT cells deficient Jα18$^{-/-}$ mice. Unexpectedly, preliminary results showed that infarct size after I/R injury tended to be decreased in Jα18$^{-/-}$ mice compared to C57BL/6J control mice (IS/AAR in I/R+vehicle group from **Figure 3** vs. IS/AAR in Jα18$^{-/-}$+I/R+vehicle group from **Supplemental Figure 4**). These results suggest that endogenously activated iNKT cells may be involved in the development of I/R injury, even though endogenous ligand for the activation of iNKT cells has never been elucidated. Therefore, the discrepancy in these results may be due to the difference in the methods to activate iNKT cells; endogenous ligand vs. exogenously administrated αGC. Finally, protein levels of several cytokines could not be detected in the heart by ELISA in the present study. This may be due to short half-life, and smaller amount of cytokines protein in the heart than in the serum.

Conclusions

Activated iNKT cells by αGC play a protective role against myocardial I/R injury through the enhanced expression of IL-10. Therapies designed to activate iNKT cells might be beneficial to protect the heart from I/R injury.

Acknowledgements

We thank Akiko Aita, Miwako Fujii and Kaoruko Naradate for excellent technical assistance.

Disclosures

None.

Funding

This study was supported by grants from the Ministry of Education, Culture, Sports, Science, and Technology of Japan (24659379, 20117004, 21390236).

References

[1] Cannon CP, Gibson CM, Lambrew CT, Shoultz DA, Levy D, French WJ, et al. Relationship of symptom-onset-to-balloon time and door-to-balloon time with mortality in patients undergoing angioplasty for acute myocardial infarction JAMA 2000;283:2941-7.

[2] Yellon DM, Hausenloy DJ. Myocardial reperfusion injury N Engl J Med 2007;357:1121-35.

[3] Zuidema MY, Zhang C. Ischemia/reperfusion injury: The role of immune cells World J Cardiol 2010;2:325-32.

[4] Hawkins HK, Entman ML, Zhu JY, Youker KA, Berens K, Dore M, et al. Acute inflammatory reaction after myocardial ischemic injury and reperfusion. Development and use of a neutrophil-specific antibody Am J Pathol 1996;148:1957-69.

[5] Yang Z, Day YJ, Toufektsian MC, Xu Y, Ramos SI, Marshall MA, et al. Myocardial infarct-sparing effect of adenosine A2A receptor activation is due to its action on CD4+ T lymphocytes Circulation 2006;114:2056-64.

[6] Birdsall HH, Green DM, Trial J, Youker KA, Burns AR, MacKay CR, et al. Complement C5a, TGF-beta 1, and MCP-1, in sequence, induce migration of monocytes into ischemic canine myocardium within the first one to five hours after reperfusion Circulation 1997;95:684-92.

[7] Frangogiannis NG, Lindsey ML, Michael LH, Youker KA, Bressler RB, Mendoza LH, et al. Resident cardiac mast cells degranulate and release preformed TNF-alpha, initiating the cytokine cascade in experimental canine myocardial ischemia/reperfusion Circulation 1998;98:699-710.

[8] Godfrey DI, MacDonald HR, Kronenberg M, Smyth MJ, Van Kaer L. NKT cells: what's in a name? Nat Rev Immunol 2004;4:231-7.

[9] Bendelac A, Savage PB, Teyton L. The biology of NKT cells Annu Rev Immunol 2007;25:297-336.

[10] Matsuda JL, Mallevaey T, Scott-Browne J, Gapin L. CD1d-restricted iNKT cells, the 'Swiss-Army knife' of the immune system Curr Opin Immunol 2008;20:358-68.

[11] Hong S, Wilson MT, Serizawa I, Wu L, Singh N, Naidenko OV, et al. The natural killer T-cell ligand alpha-galactosylceramide prevents autoimmune diabetes in non-obese diabetic mice Nat Med 2001;7:1052-6.

[12] Sharif S, Arreaza GA, Zucker P, Mi QS, Sondhi J, Naidenko OV, et al. Activation of natural killer T cells by alpha-galactosylceramide treatment prevents the onset and recurrence of autoimmune Type 1 diabetes Nat Med 2001;7:1057-62.

[13] Singh AK, Wilson MT, Hong S, Olivares-Villagomez D, Du C, Stanic AK, et al. Natural killer T cell activation protects mice against experimental autoimmune encephalomyelitis J Exp Med 2001;194:1801-11.

[14] Miellot A, Zhu R, Diem S, Boissier MC, Herbelin A, Bessis N. Activation of invariant NK T cells protects against experimental rheumatoid arthritis by an IL-10-dependent pathway Eur J Immunol 2005;35:3704-13.

[15] Ronet C, Darche S, Leite de Moraes M, Miyake S, Yamamura T, Louis JA, et al. NKT cells are critical for the initiation of an inflammatory bowel response against Toxoplasma gondii J Immunol 2005;175:899-908.

[16] Kawano T, Cui J, Koezuka Y, Toura I, Kaneko Y, Motoki K, et al. CD1d-restricted and TCR-mediated activation of valpha14 NKT cells by glycosylceramides Science 1997;278:1626-9.

[17] Sobirin MA, Kinugawa S, Takahashi M, Fukushima A, Homma T, Ono T, et al. Activation of natural killer T cells ameliorates postinfarct cardiac remodeling and failure in mice Circ Res 2012;111:1037-47.

[18] Cao Z, Yuan Y, Jeyabalan G, Du Q, Tsung A, Geller DA, et al. Preactivation of NKT cells with alpha-GalCer protects against hepatic ischemia-reperfusion injury in mouse by a mechanism involving IL-13 and adenosine A2A receptor Am J Physiol Gastrointest Liver Physiol 2009;297:G249-58.

[19] Crowe NY, Uldrich AP, Kyparissoudis K, Hammond KJ, Hayakawa Y, Sidobre S, et al. Glycolipid antigen drives rapid expansion and sustained cytokine production by NK T cells J Immunol 2003;171:4020-7.

[20] Miellot A, Zhu R, Diem S, Boissier MC, Herbelin A, Bessis N. Activation of invariant NK T cells protects against experimental rheumatoid arthritis by an IL-10-dependent pathway Eur J Immunol 2005;35:3704-13.

[21] Mabalirajan U, Dinda AK, Kumar S, Roshan R, Gupta P, Sharma SK, et al. Mitochondrial structural changes and dysfunction are associated with experimental allergic asthma J Immunol 2008;181:3540-8.

[22] Miyamoto K, Miyake S, Yamamura T. A synthetic glycolipid prevents autoimmune encephalomyelitis by inducing TH2 bias of natural killer T cells Nature 2001;413:531-4.

[23] Parekh VV, Singh AK, Wilson MT, Olivares-Villagomez D, Bezbradica JS, Inazawa H, et al. Quantitative and qualitative differences in the in vivo response of NKT cells to distinct alpha- and beta-anomeric glycolipids J Immunol 2004;173:3693-706.

[24] Duan W, Yang Y, Yan J, Yu S, Liu J, Zhou J, et al. The effects of curcumin post-treatment against myocardial ischemia and reperfusion by activation of the JAK2/STAT3 signaling pathway Basic Res Cardiol;107:263.

[25] Bharti S, Golechha M, Kumari S, Siddiqui KM, Arya DS. Akt/GSK-3beta/eNOS phosphorylation arbitrates safranal-induced myocardial protection against ischemia-reperfusion injury in rats Eur J Nutr;51:719-27.

[26] Van Kaer L. alpha-Galactosylceramide therapy for autoimmune diseases: prospects and obstacles Nat Rev Immunol 2005;5:31-42.

[27] Wilson MT, Johansson C, Olivares-Villagomez D, Singh AK, Stanic AK, Wang CR, et al. The response of natural killer T cells to glycolipid antigens is characterized by surface receptor down-modulation and expansion Proc Natl Acad Sci U S A 2003;100:10913-8.

[28] Aoyagi T, Yamamoto N, Hatta M, Tanno D, Miyazato A, Ishii K, et al. Activation of pulmonary invariant NKT cells leads to exacerbation of acute lung injury caused by LPS through local production of IFN-gamma and TNF-alpha by Gr-1+ monocytes Int Immunol 2011;23:97-108.

[29] Li L, Huang L, Vergis AL, Ye H, Bajwa A, Narayan V, et al. IL-17 produced by neutrophils regulates IFN-gamma-mediated neutrophil migration in mouse kidney ischemia-reperfusion injury J Clin Invest 2010;120:331-42.

[30] Frangogiannis NG, Youker KA, Rossen RD, Gwechenberger M, Lindsey MH, Mendoza LH, et al. Cytokines and the microcirculation in ischemia and reperfusion J Mol Cell Cardiol 1998;30:2567-76.

[31] Zhang M, Chen L. Status of cytokines in ischemia reperfusion induced heart injury Cardiovasc Hematol Disord Drug Targets 2008;8:161-72.

[32] Gurevitch J, Frolkis I, Yuhas Y, Lifschitz-Mercer B, Berger E, Paz Y, et al. Anti-tumor necrosis factor-alpha improves myocardial recovery after ischemia and reperfusion J Am Coll Cardiol 1997;30:1554-61.

[33] Venkatachalam K, Prabhu SD, Reddy VS, Boylston WH, Valente AJ, Chandrasekar

B. Neutralization of interleukin-18 ameliorates ischemia/reperfusion-induced myocardial injury J Biol Chem 2009;284:7853-65.

[34] Yang Z, Zingarelli B, Szabo C. Crucial role of endogenous interleukin-10 production in myocardial ischemia/reperfusion injury Circulation 2000;101:1019-26.

[35] Hayward R, Nossuli TO, Scalia R, Lefer AM. Cardioprotective effect of interleukin-10 in murine myocardial ischemia-reperfusion Eur J Pharmacol 1997;334:157-63.

[36] Manukyan MC, Alvernaz CH, Poynter JA, Wang Y, Brewster BD, Weil BR, et al. Interleukin-10 protects the ischemic heart from reperfusion injury via the STAT3 pathway Surgery 2011;150:231-9.

[37] Lefer AM, Ma XL, Weyrich AS, Scalia R. Mechanism of the cardioprotective effect of transforming growth factor beta 1 in feline myocardial ischemia and reperfusion Proc Natl Acad Sci U S A 1993;90:1018-22.

[38] Ito S, Ansari P, Sakatsume M, Dickensheets H, Vazquez N, Donnelly RP, et al. Interleukin-10 inhibits expression of both interferon alpha- and interferon gamma- induced genes by suppressing tyrosine phosphorylation of STAT1 Blood 1999;93:1456-63.

[39] Moore KW, de Waal Malefyt R, Coffman RL, O'Garra A. Interleukin-10 and the interleukin-10 receptor Annu Rev Immunol 2001;19:683-765.

[40] Kopydlowski KM, Salkowski CA, Cody MJ, van Rooijen N, Major J, Hamilton TA, et al. Regulation of macrophage chemokine expression by lipopolysaccharide in vitro and in

vivo J Immunol 1999;163:1537-44.

[41] Cai ZP, Parajuli N, Zheng X, Becker L. Remote ischemic preconditioning confers late protection against myocardial ischemia-reperfusion injury in mice by upregulating interleukin-10 Basic Res Cardiol 2012;107:277.

[42] Krishnamurthy P, Rajasingh J, Lambers E, Qin G, Losordo DW, Kishore R. IL-10 inhibits inflammation and attenuates left ventricular remodeling after myocardial infarction via activation of STAT3 and suppression of HuR Circ Res 2009;104:e9-18.

[43] Krown KA, Page MT, Nguyen C, Zechner D, Gutierrez V, Comstock KL, et al. Tumor necrosis factor alpha-induced apoptosis in cardiac myocytes. Involvement of the sphingolipid signaling cascade in cardiac cell death J Clin Invest 1996;98:2854-65.

[44] McTiernan CF, Lemster BH, Frye C, Brooks S, Combes A, Feldman AM. Interleukin-1 beta inhibits phospholamban gene expression in cultured cardiomyocytes Circ Res 1997;81:493-503.

[45] Giaccone G, Punt CJ, Ando Y, Ruijter R, Nishi N, Peters M, et al. A phase I study of the natural killer T-cell ligand alpha-galactosylceramide (KRN7000) in patients with solid tumors Clin Cancer Res 2002;8:3702-9.

[46] Nieda M, Okai M, Tazbirkova A, Lin H, Yamaura A, Ide K, et al. Therapeutic activation of Valpha24+Vbeta11+ NKT cells in human subjects results in highly coordinated secondary activation of acquired and innate immunity Blood 2004;103:383-9.

[47] Ishikawa A, Motohashi S, Ishikawa E, Fuchida H, Higashino K, Otsuji M, et al. A phase I study of alpha-galactosylceramide (KRN7000)-pulsed dendritic cells in patients with advanced and recurrent non-small cell lung cancer Clin Cancer Res 2005;11:1910-7.

[48] Uchida T, Horiguchi S, Tanaka Y, Yamamoto H, Kunii N, Motohashi S, et al. Phase I study of alpha-galactosylceramide-pulsed antigen presenting cells administration to the nasal submucosa in unresectable or recurrent head and neck cancer Cancer Immunol Immunother 2008;57:337-45.

[49] Motohashi S, Nagato K, Kunii N, Yamamoto H, Yamasaki K, Okita K, et al. A phase I-II study of alpha-galactosylceramide-pulsed IL-2/GM-CSF-cultured peripheral blood mononuclear cells in patients with advanced and recurrent non-small cell lung cancer J Immunol 2009;182:2492-501.

[50] Barral P, Sanchez-Nino MD, van Rooijen N, Cerundolo V, Batista FD. The location of splenic NKT cells favours their rapid activation by blood-borne antigen EMBO J 2012;31:2378-90.

[51] Sonoda KH, Faunce DE, Taniguchi M, Exley M, Balk S, Stein-Streilein J. NK T cell-derived IL-10 is essential for the differentiation of antigen-specific T regulatory cells in systemic tolerance J Immunol 2001;166:42-50.

Table 1. Echocardiogram and Hemodynamics 28 days after reperfusion

	I/R+vehicle	I/R+αGC
Echocardiography	n=8	n=8
LVEDD, mm	3.7±0.1	3.5±0.1
LVESD, mm	3.0±0.1	2.7±0.1†
FS, %	18.9±0.9	24.0±1.1†
AWT, mm	0.64±0.02	0.71±0.01†
PWT, mm	0.80±0.02	0.82±0.02
Hemodynamics	n=6	n=7
Heart rate, bpm	456±25	449±20
Systolic BP, mmHg	108.2±6.2	108.1±3.7
Diastolic BP, mmHg	78.8±4.7	76.5±1.9
LVEDP, mmHg	5.2±0.4	1.9±0.3†
LV +dP/dt, mmHg/s	10633±1824	11841±1284
LV –dP/dt, mmHg/s	7365±1600	7286±1105

LVEDD indicates left ventricular end-diastolic diameter; LVESD, left ventricular end-systolic diameter; FS, fractional shortening; AWT, anterior wall thickness; PWT, posterior wall thickness; BP, blood pressure; LVEDP, left ventricular end-diastolic pressure. Data are expressed as means±SE. † $P<0.05$ vs. I/R+vehicle.

Figure Legends

Figure 1. Specificity of αGC for iNKT cells

(A) Serum levels of IL-10, IL-4 and IFN-γ at 0, 0.5, 1, 3, 6, 12 and 24 hr after αGC intraperitoneal injection into Jα18$^{-/-}$ mice (0.1 μg/g body weight). n=3 for each group. **(B)** Quantitative analysis of IL-10, IL-4 and IFN-γ mRNA expression in the myocardium after αGC injection into Jα18$^{-/-}$ mice. n=3 for each group. Data are expressed as means±SE. * P<0.05 vs. 0 hr. ND, not detected.

Figure 2. The proportion of iNKT cells in the heart from 4 groups of mice

(A) Representative flow cytometric analyses of cardiac mononuclear cell (MNC) suspensions 72 hr after reperfusion from Sham+vehicle, Sham+αGC, I/R+vehicle and I/R+αGC. Cardiac MNCs from 3 different mice for each group were pooled and analyzed. Circles indicate the population of iNKT cells. **(B)** Summary data for the proportion of iNKT cells. n=3 for each group. Data are expressed as means±SE. * P<0.05 vs. Sham+vehicle. † P<0.05 vs. I/R+vehicle.

Figure 3. Effects of αGC on myocardial I/R injury at 24hr

(A) Representative pictures of Evans Blue and TTC–stained LV sections from I/R+vehicle and I/R+αGC (upper panels). IS/AAR and AAR/LV 24 hr after reperfusion in I/R+vehicle (n=16) and I/R+αGC (n=14) mice (lower panel). **(B)** Serum levels of troponin-I 24 hr after reperfusion in

Sham+vehicle (n=8), Sham+αGC (n=8), I/R+vehicle (n=16) and I/R+αGC (n=14) mice. Data are expressed as means±SE. * $P<0.05$ vs. Sham+vehicle. † $P<0.05$ vs. I/R+vehicle. ND, not detected.

Figure 4. Effects of αGC on the number of infiltrating inflammatory cells in ischemic myocardium

(A) Representative photomicrographs of LV sections stained with anti-myeloperoxidase (MPO), anti-CD3 and anti-MAC3 24 hr after reperfusion. **(B)** Summary data for the number of MPO-positive cells and CD3-positive cells and the ratio of MAC3-positive area. n=7-8 for each group. Data are expressed as means±SE. * $P<0.05$ vs. Sham+vehicle. † $P<0.05$ vs. I/R+vehicle. HPF, high power field.

Figure 5. Effects of αGC on apoptosis

(A) Representative photomicrographs of TUNEL-stained LV sections. TUNEL-positive nuclei (green), myoglobin (red), and DAPI (blue). Arrows indicate TUNEL-positive cells. **(B)** Summary data for the number of TUNEL-positive cells. n=7-8 for each group. **(C)** Representative immunoblotting analysis and the summary data for caspase-3/GAPDH. n=6 for each group. Data are expressed as means±SE. * $P<0.05$ vs. Sham+vehicle. † $P<0.05$ vs. I/R+vehicle.

Figure 6. Effects of αGC on serum levels and myocardial gene expression of cytokines

(A) Serum levels of IL-10, IL-4 and IFN-γ 24 hr after reperfusion. **(B)** Quantitative analysis of mRNA expression of IL-10, IL-4, IFN-γ, TNF-α, IL-1β, and TGF-β1 in ischemic myocardium 24 hr after reperfusion. n=8 for each group. Data are expressed as means±SE. * $P<0.05$ vs. Sham+vehicle. † $P<0.05$ vs. I/R+vehicle. ND, not detected.

Figure 7. Effects of neutralizing antibodies on αGC-induced amelioration of I/R injury

Representative pictures of Evans Blue and TTC–stained LV sections from I/R+αGC+rat IgG1κ, I/R+αGC+anti-IL-10 receptor mAb (IL-10R), I/R+αGC+anti-IL-4 mAb and I/R+αGC+anti-IFN-γ mAb (upper panels). Summary data for IS/AAR and AAR/LV 24 hr of reperfusion (lower panel). n=7-9 for each group. Data are expressed as means±SE. * $P<0.05$ vs I/R+αGC+rat IgG1κ.

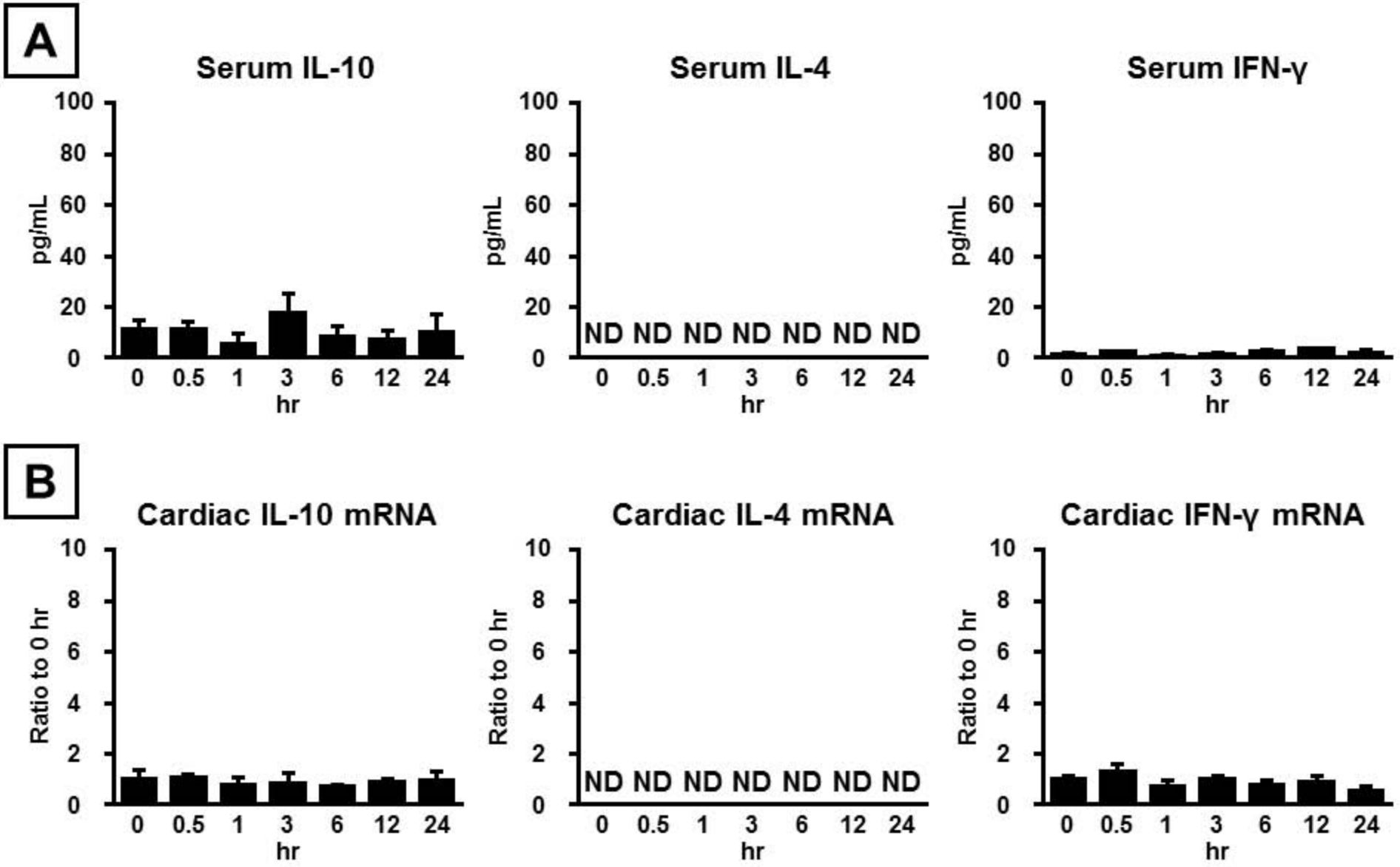
A
Serum IL-10
Serum IL-4
Serum IFN-γ
pg/mL
100
80
60
40
20
0
ND ND ND ND ND ND ND
0 0.5 1 3 6 12 24
hr
B
Cardiac IL-10 mRNA
Cardiac IL-4 mRNA
Cardiac IFN-γ mRNA
Ratio to 0 hr
10
8
6
4
2
0

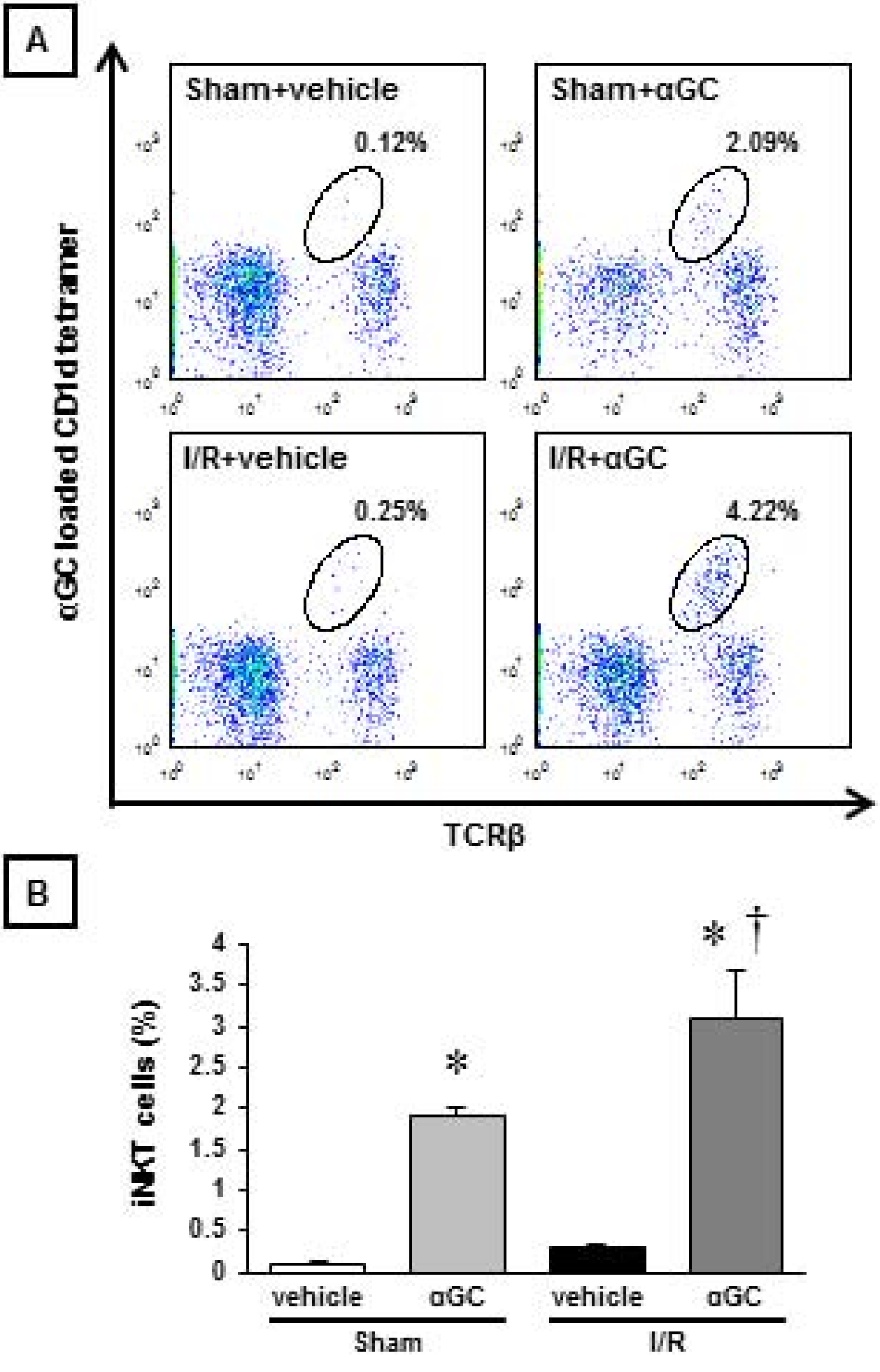
A
Sham+vehicle
0.12%
Sham+αGC
2.09%
I/R+vehicle
0.25%
I/R+αGC
4.22%
αGC loaded CD1d tetramer
TCRβ
B
iNKT cells (%)
4
3.5
3
2.5
2
1.5
1
0.5
0
*
* †
vehicle
αGC
vehicle
αGC
Sham
I/R

A

I/R+vehicle

I/R+αGC

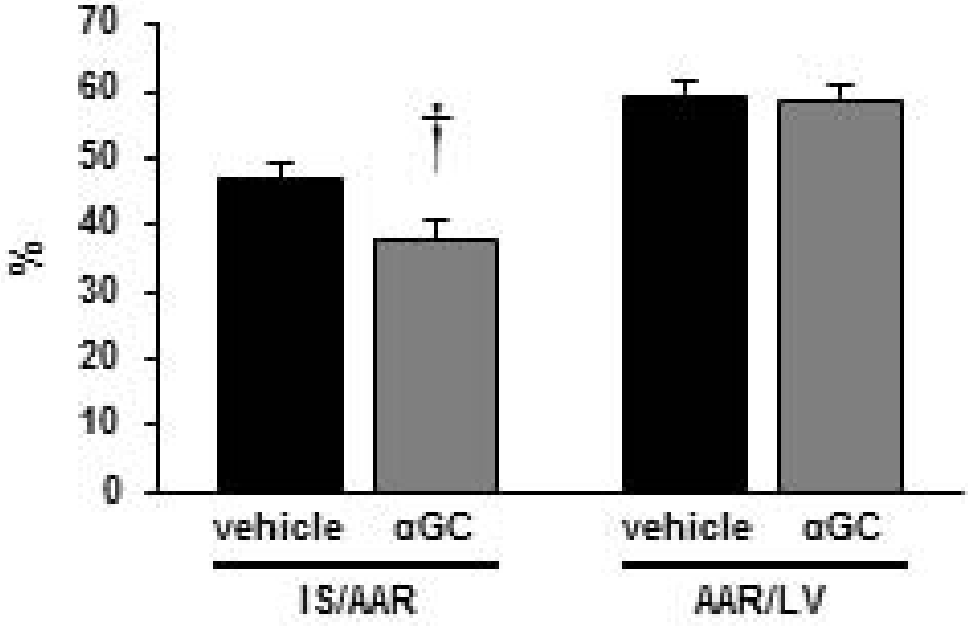

B

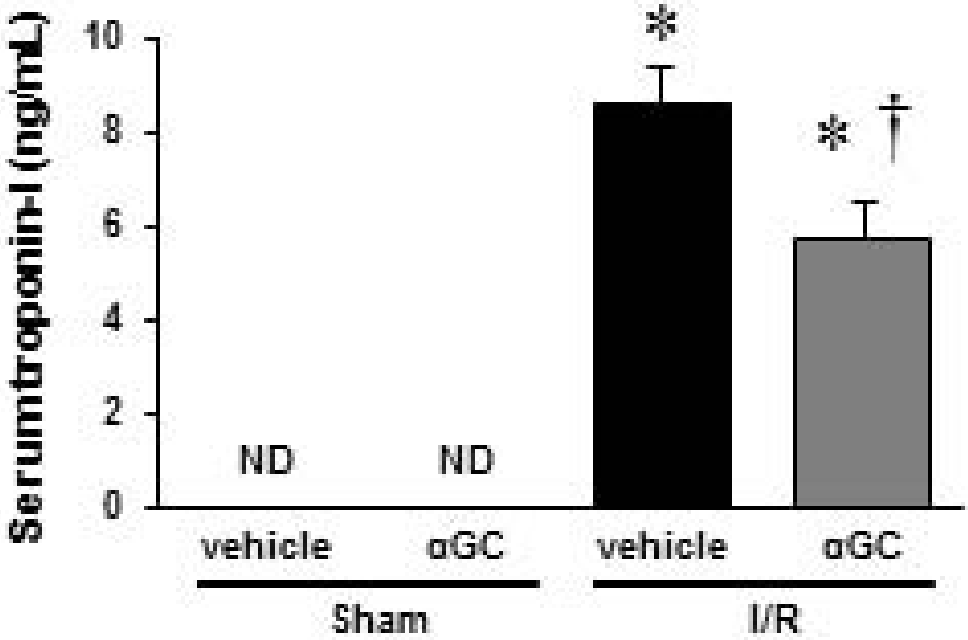

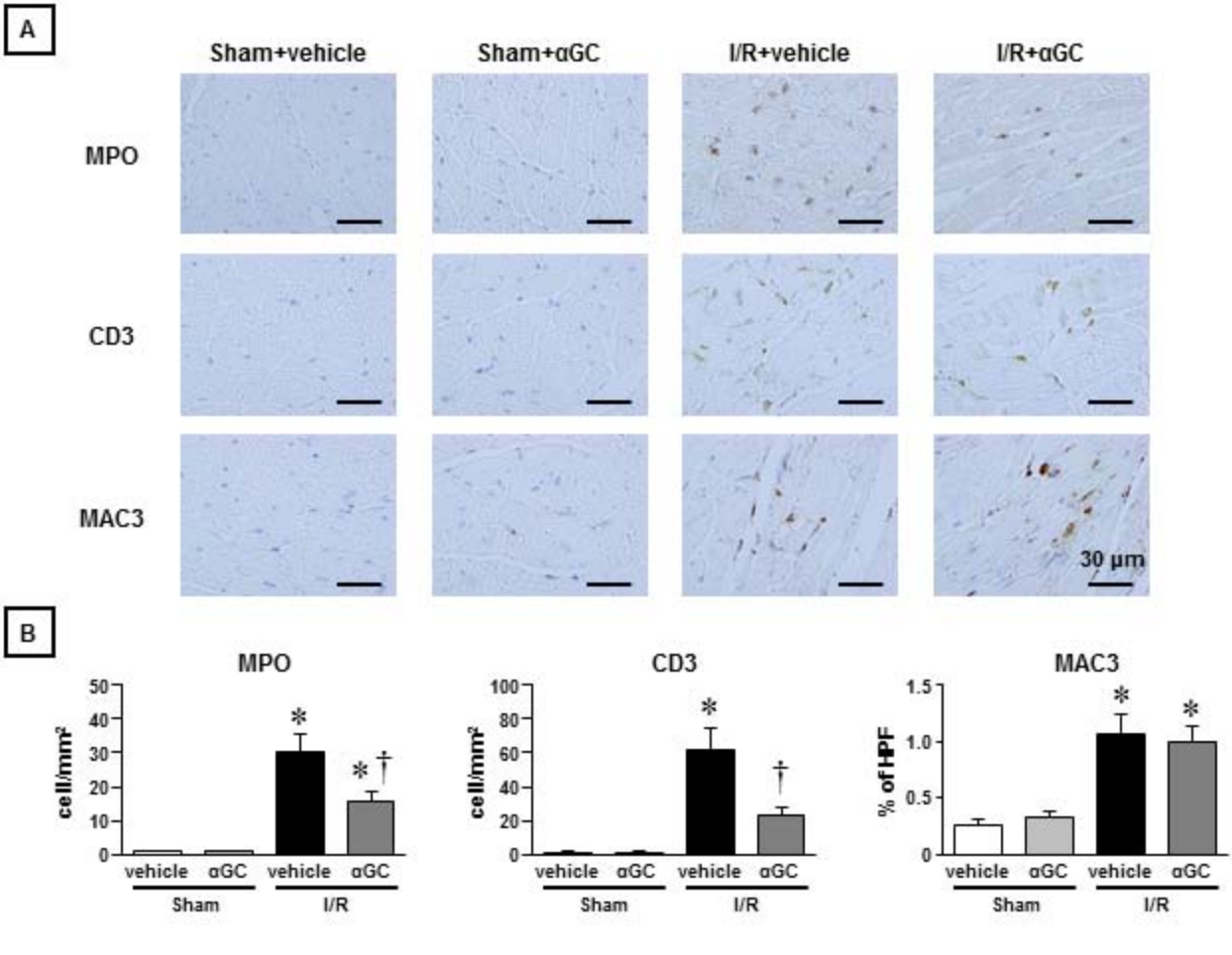
A
Sham+vehicle
Sham+αGC
I/R+vehicle
I/R+αGC
MPO
CD3
MAC3
30 μm
B
MPO
cell/mm²
50
40
30
20
10
0
vehicle
αGC
vehicle
αGC
Sham
I/R
CD3
cell/mm²
100
80
60
40
20
0
vehicle
αGC
vehicle
αGC
Sham
I/R
MAC3
% of HPF
1.5
1.0
0.5
0
vehicle
αGC
vehicle
αGC
Sham
I/R

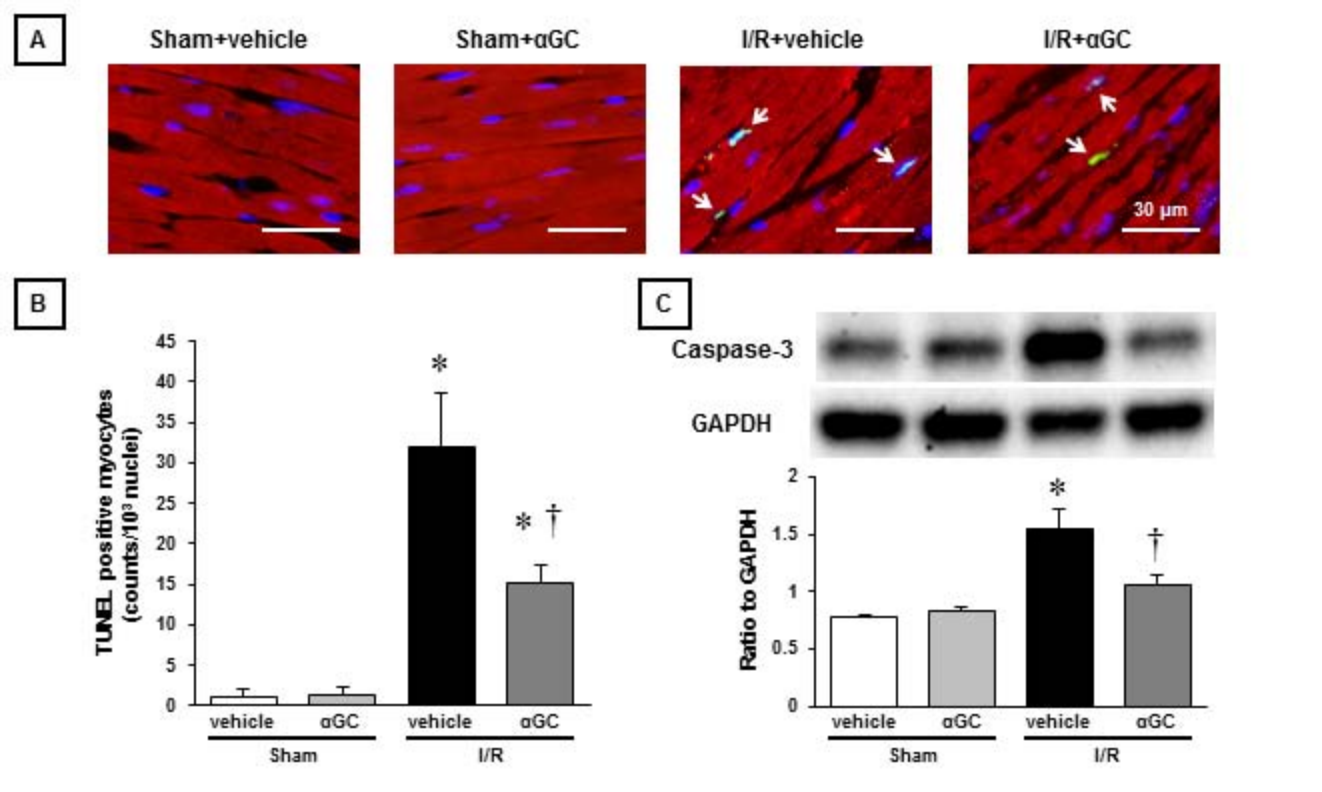
A
Sham+vehicle
Sham+αGC
I/R+vehicle
I/R+αGC
30 μm
B
TUNEL positive myocytes (counts/10³ nuclei)
45
40
35
30
25
20
15
10
5
0
*
* †
vehicle
αGC
vehicle
αGC
Sham
I/R
C
Caspase-3
GAPDH
Ratio to GAPDH
2
1.5
1
0.5
0
*
†
vehicle
αGC
vehicle
αGC
Sham
I/R

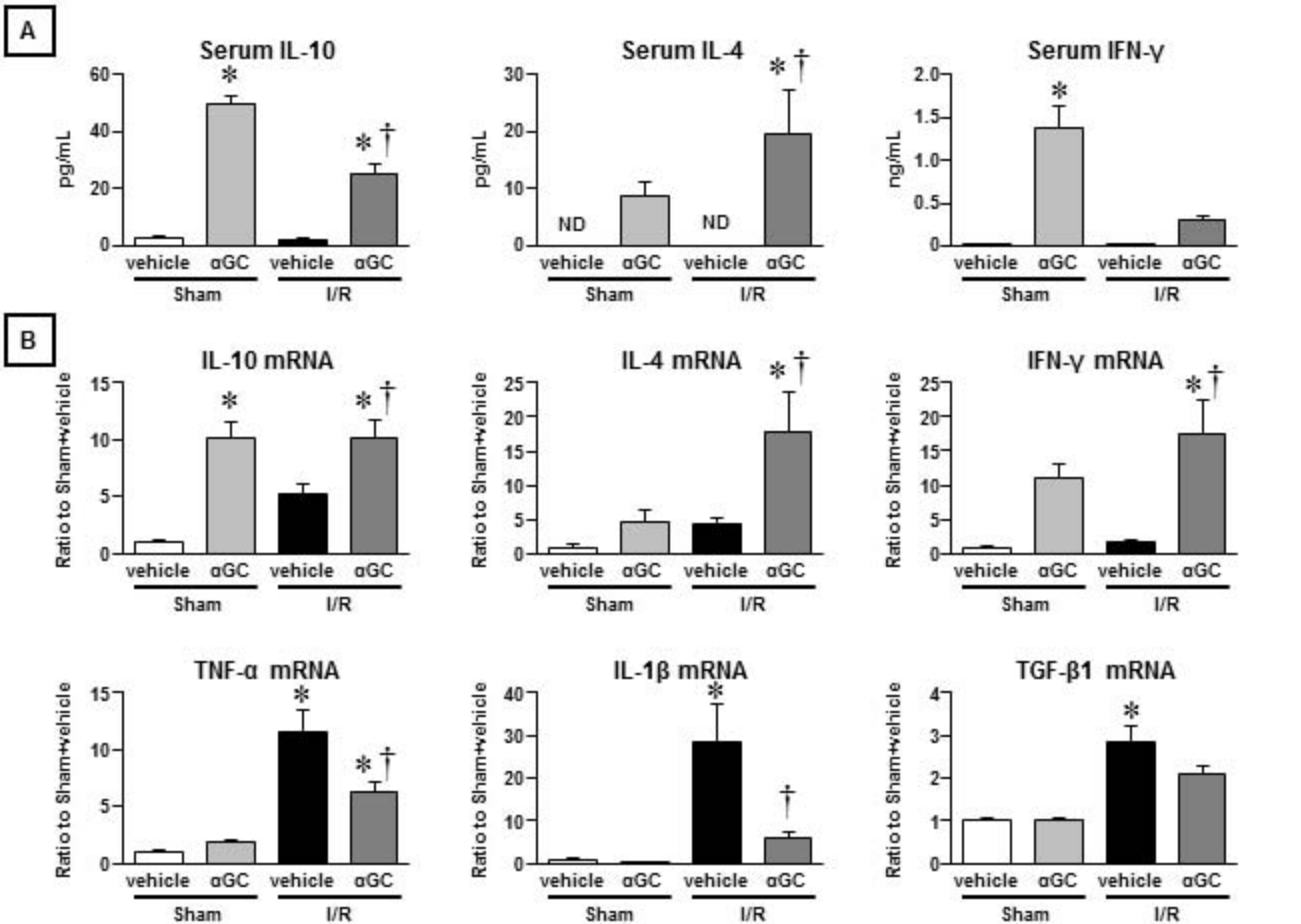
A
Serum IL-10
pg/mL
60
40
20
0
*
*†
vehicle
αGC
vehicle
αGC
Sham
I/R
Serum IL-4
pg/mL
30
20
10
0
ND
ND
*†
vehicle
αGC
vehicle
αGC
Sham
I/R
Serum IFN-γ
ng/mL
2.0
1.5
1.0
0.5
0
*
vehicle
αGC
vehicle
αGC
Sham
I/R
B
IL-10 mRNA
Ratio to Sham+vehicle
15
10
5
0
*
*†
vehicle
αGC
vehicle
αGC
Sham
I/R
IL-4 mRNA
Ratio to Sham+vehicle
25
20
15
10
5
0
*†
vehicle
αGC
vehicle
αGC
Sham
I/R
IFN-γ mRNA
Ratio to Sham+vehicle
25
20
15
10
5
0
*†
vehicle
αGC
vehicle
αGC
Sham
I/R
TNF-α mRNA
Ratio to Sham+vehicle
15
10
5
0
*
*†
vehicle
αGC
vehicle
αGC
Sham
I/R
IL-1β mRNA
Ratio to Sham+vehicle
40
30
20
10
0
*
†
vehicle
αGC
vehicle
αGC
Sham
I/R
TGF-β1 mRNA
Ratio to Sham+vehicle
4
3
2
1
0
*
vehicle
αGC
vehicle
αGC
Sham
I/R

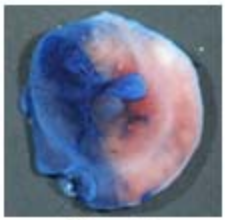

I/R+αGC
+rat IgG1κ

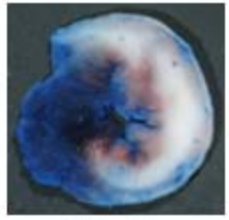

I/R+αGC
+anti-IL-10R

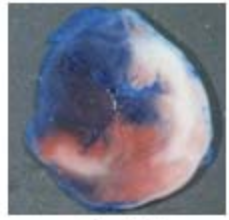

I/R+αGC
+anti-IL-4

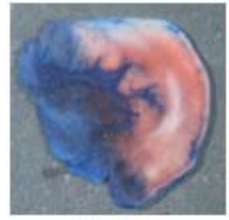

I/R+αGC
+anti-IFN-γ

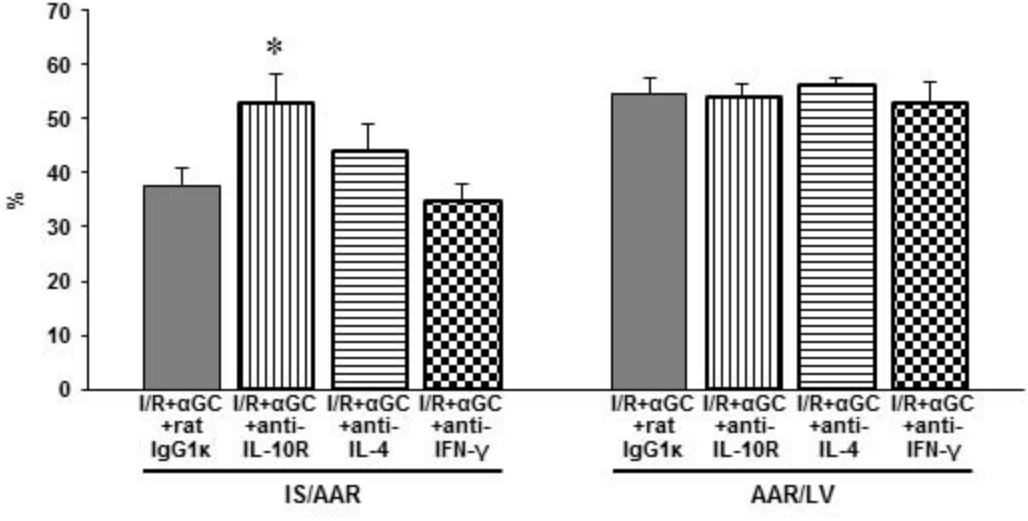

Supplementary Material

Detailed Methods

1. Anesthesia

Mice were anaesthetized with pentobarbital (50 μg/g body weight i.p.) throughout the experiments, and its adequacy was monitored from the disappearance of the pedal withdrawal reflex.

2. Flow Cytometric Analysis of Cardiac and Splenic Mononuclear Cells

LV tissues were harvested, minced with a fine scissors, placed in 10 mL RPMI-1640 (Sigma-Aldrich, St. Louis, MO) with 5% fetal bovine serum (FBS, Sigma-Aldrich), 1 mg/mL collagenase type IV (Sigma-Aldrich), and 100 U/mL DNase I (Sigma-Aldrich), shaken at 37°C for 45 min, and then triturated through 70 μm nylon mesh and centrifuged. Red blood cells were lysed with Tris-ammonium chloride for 1 min at room temperature. Cardiac mononuclear cells (MNCs) were isolated by density-gradient centrifugation with 12 mL of 33% Percoll^{TM} (Sigma-Aldrich), as previously described [1]. Cardiac MNCs from 3 mice were pooled, and subjected to flow cytometric analysis.

Spleens were harvested and triturated through 70 μm nylon mesh. After centrifugation, splenic MNCs were isolated by lysis of red blood cells with Tris-ammonium chloride for 1 min at room temperature.

To detect cardiac iNKT cells, below procedures were performed. Cardiac and splenic MNCs were incubated with 2.4G2 monoclonal antibody to block non-specific binding of primary monoclonal antibody. After washing, cells were stained with a combination of fluorescein isothiocyanate (FITC) conjugated anti-mouse TCR-β (BD Pharmingen), allophycocyanin (APC) conjugated anti-mouse NK1.1 (BD Pharmingen), BD Horizon^{TM} V-450 conjugated anti-mouse CD45 (BD Pharmingen), and R-phycoerythrin (R-PE) conjugated αGC-loaded murine CD1d tetramer (ProImmune, Oxford, UK). Cells were washed and propidium iodide (PI, Sigma-Aldrich) was added to distinguish dead cells. Stained cells were acquired with FACS Canto II Flow Cytometer (BD Biosciences Immunocytometry Systems, San Jose, CA) and analyzed with FlowJo ver.7.2.5 (Tommy Digital Biology, Tokyo, Japan). CD45-positive and PI-negative cells were gated to identify live leukocytes. Each sample population was classified for cell size (forward scatter) and complexity (side scatter), then gated on a population of lymphocytes. In this population, CD1d tetramer^{+}TCR-β^{+} cells were identified as iNKT cells.

To measure infiltrating neutrophils and macrophages in the ischemic heart, cardiac MNCs were stained with PE conjugated anti-mouse Ly-6G (BD Pharmingen) and BD Horizon^{TM} V-450 conjugated anti-mouse CD45. After washing, cells were fixed and permeabilizated by Foxp3 / Transcription Factor Staining Buffer Set (eBioschience, Inc., San Diego, CA). Cells were washed and stained with APC conjugated anti-mouse CD68 (BioLegend, Inc., San Diego, CA). CD45^{+} cells were identified as leukocytes, CD45^{+}Ly6G^{+} cells as neutrophils, and CD45^{+}CD68^{+} cells as macrophages/monocytes. In CD45^{+}CD68^{+} cells, we gated on monocyte subsets by forward scatter and

side scatter, and excluded this population to identify macrophages. Reported cell numbers were calculated as the product of living MNCs and percentage of each population.

To identify Ly6C high macrophages/monocytes, cardiac MNCs were stained with V-450 conjugated anti-mouse CD45, FITC conjugated anti-mouse CD11b, APC conjugated Ly6C, and PE conjugated anti-mouse Ly6G, CD90.2, B220, and NK1.1 (all antibodies were purchased from BD Pharmingen). Cells were washed and PI was added to distinguish dead cells. CD45-positive, PI-negative, (Ly6G, CD90.2, B220, and NK1.1)-negative, and CD11b positive cells were gated to identify live macrophages/monocytes. In this population, we gated on monocyte subsets by forward scatter and side scatter. Ly6C high cells were identified as Ly6C high monocytes.

3. ELISA

Blood samples were allowed to clot for 2 hr at room temperature and then centrifuged for 20 min at 2000 *g*. Serum IL-10, IL-4, IFN-γ, and troponin-I levels were measured by commercially available ELISA kit (IL-10, IL-4, and IFN-γ, R&D Systems, Inc.; troponin-I, Life Diagnostics, Inc., West Chester, PA) according to the manufacturer's instructions. In troponin-I ELISA kit, 100 ml of cTnI HRP Conjugate and 100 ml of standards or samples were added to each well and incubated for 60 min at room temperature. After washing each well, 100 ml of TMB Reagent was added to each well and incubated for 20 min at room temperature. The reaction was stopped by adding 100 ml of Stop Solution to each well. We read absorbance at 450 nm with a plate reader and calculated the

corresponding concentration of troponin-I (ng/ml) from the standard curve.

4. qRT-PCR

Total RNA was extracted from myocardium with QuickGene-810 (FujiFilm, Tokyo, Japan) according to the manufacturer's instructions. In I/R mice, ischemic myocardium was used. cDNA was synthesized with the high capacity cDNA reverse transcription kit (Applied Biosystems, Foster City, CA). TaqMan quantitative PCR was performed with the 7300 real-time PCR system (Applied Biosystems) to amplify samples for IL-10, IL-4, IFN-γ, tumor necrosis factor (TNF)-α, IL-1β, transforming growth factor (TGF)-β1, monocyte chemotactic protein-1 (MCP-1), intercellular adhesion molecule-1 (ICAM-1), and vascular cell adhesion molecule-1 (VCAM-1). These transcripts were normalized to GAPDH. All primers were purchased from Applied Biosystems.

5. Infarct Size

The mice were euthanized 24 hr after reperfusion. Trachea incubation was performed and mechanical ventilation was established. A left thoracotomy was performed and the left coronary artery was reoccluded at the same level with an 8-0 suture and 4% Evans Blue (Wako, Osaka, Japan) was injected via inferior vena cava to determine area at risk (AAR). The hearts were immediately excised and rinsed in ice-cold PBS. The hearts were cut into 5 transverse slices and incubated in 1.5% 2,3,5-triphenyltetrazolium chloride (TTC, Wako) for 15 min at 37°C to determine infarct size (IS).

Heart slices were digitally photographed under a microscope. IS, AAR, and total LV area were measured with ImageJ software (version 1.44).

6. Immunohistochemical Analysis of Inflammatory Cells

The hearts were harvested 24 hr after reperfusion and immediately fixed in 4% paraformaldehyde in PBS (pH 7.4) for paraffin embedding. Paraffin-embedded sections were pretreated with heat-induced epitope retrieval. These sections were stained for neutrophils (rabbit anti-human myeloperoxidase (MPO), 1:1000, DakoCytomation, Glostrup, Denmark), T lymphocytes (rabbit anti-human CD3, 1:100, DakoCytomation), and macrophages (rat anti-mouse MAC3, 1:20, BD Phamingen). The avidin-biotin peroxidase method was used for immunohistochemistry. The reaction was visualized with a 3-3'-diaminobenzidine (DAB) Substrate-Chromogen. All sections were counterstained with Mayer's haematoxylin. In 5 fields for each heart, the number of MPO- and CD3-positive cells was counted and the ratio of MAC3-positive area was measured with ImageJ software.

7. TUNEL Staining

Paraffin-embedded sections were pretreated with Proteinase K (400 μg/mL, 15 min, Takara Bio Inc., Otsu, Japan). Then, TUNEL staining was performed by *in situ* apoptosis detection kit (Takara Bio Inc.) according to the manufacturer’s instructions. These sections were stained with rabbit

anti-human myoglobin (1:1000, DakoCytomation, Glostrup, Denmark) and the reaction was visualized with Alexa Fluor® 555-conjugated goat anti-rabbit IgG (Molecular Probes, Inc., Glostrup, Denmark). These sections were mounted with ProLong® Gold antifade reagent with DAPI (Molecular Probes, Inc.).

8. Caspase-3 Protein

LV tissues (20 mg) were homogenized on ice in cell lysis buffer (Cell Signaling Technology, Beverly, MA) supplemented with Complete Protease Inhibitor Cocktail (Roche, Basel, Switzerland). The homogenized solution was sonicated (5 sec) and shaken for 30 min at 4°C. After centrifugation at 15000 *g* for 20 min at 4°C, the supernatants were collected. The protein concentration was quantified by the BCA Protein Assay (Pierce, Rockford, IL). Twenty micrograms of proteins were then electrophoretically separated on 10% SDS-PAGE in the Western running buffer (70 mM Tris, 192 mM glycine, 0.1% w/v SDS, and 20% v/v methanol, pH 8.3), transferred onto polyvinylidene difluoride (PVDF) membranes, and blocked with 3% nonfat dry milk. The membrane was then incubated with antibody against caspase-3 (1:1000, Cell Signaling Technology) for overnight at 4°C. Horseradish peroxidase-conjugated secondary antibodies were used for the secondary detection (1:1000, Santa Cruz Biotechnology, California, CA). The bands were revealed by the enhanced chemiluminescence (ECL) Western blotting detection reagents (Amersham Pharmacia Biotech, Bucks, UK).

Quantification of protein levels was performed with Image J. Equal loading of protein was verified by immunoblotting with GAPDH (Cell Signaling, Technology).

9. Echocardiographic and Hemodynamic Measurements

Echocardiographic and hemodynamic measurements were performed under light anesthesia with tribromoethanol/amylene hydrate (avertin; 2.5% wt/vol, 8 μL/g ip) with known short duration of action and modest cardiodepressive effects. A two-dimensional parasternal short-axis view was obtained at the levels of the papillary muscles. Two-dimensional targeted M-mode tracings were recorded at a paper speed of 50mm/s. A 1.4-Fr micromanometer-tipped catheter (Millar Instruments, Houston, Tex) was inserted into the right carotid artery and then advanced into the LV to measure LV pressures.

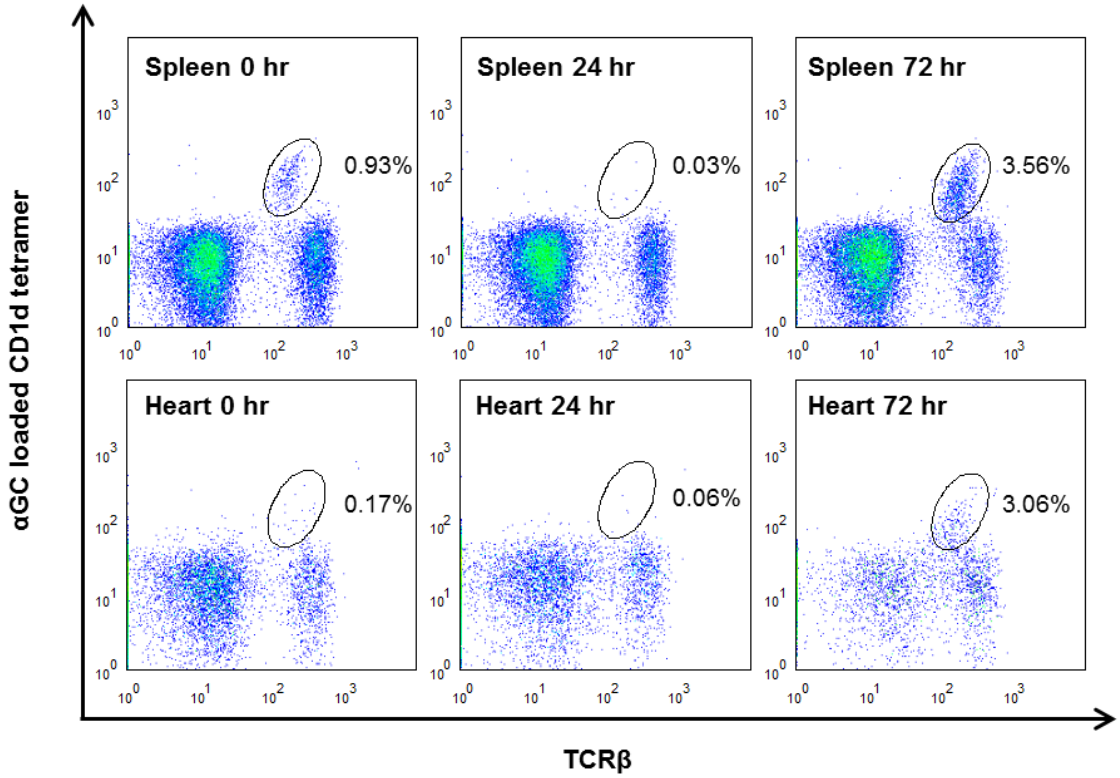

Supplemental Figure 1. Effects of αGC on splenic and cardiac iNKT cell proportion

Representative flow cytometric analyses of splenic and cardiac MNC suspensions 0, 24 and 72 hr after reperfusion αGC injection into normal mice. Cardiac MNCs from 3 different mice for each group were pooled and analysed. Circles indicate the population of iNKT cells.

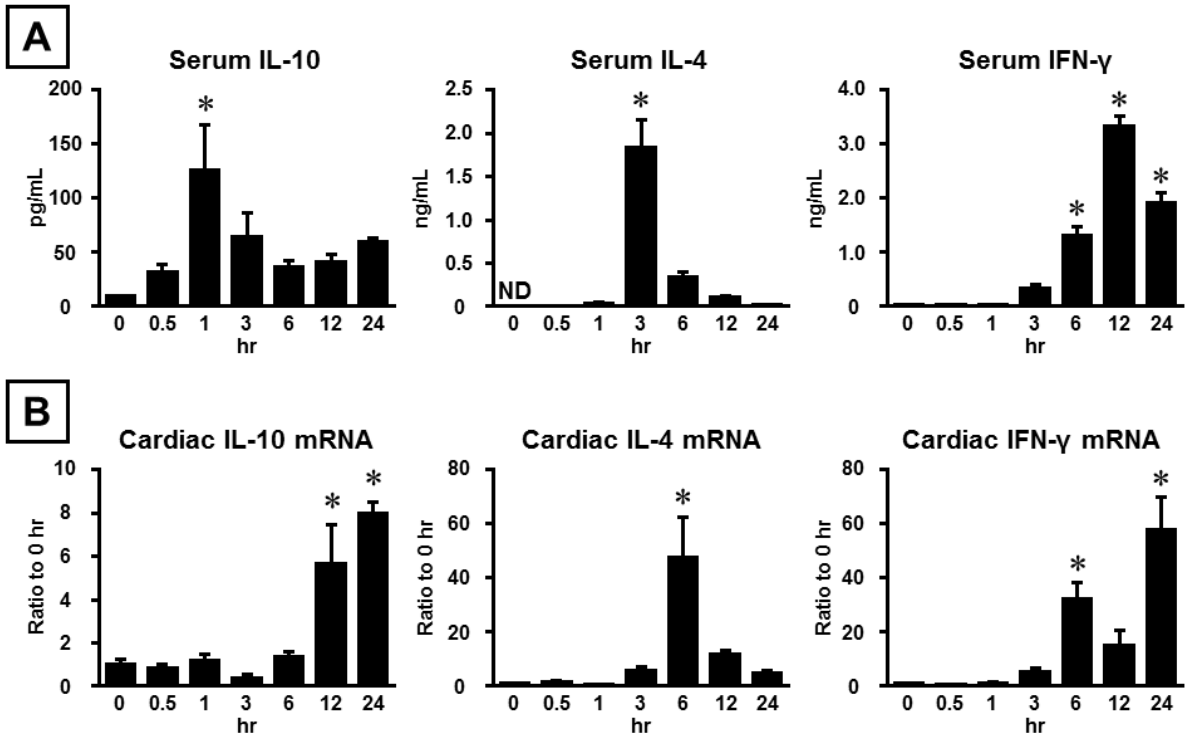

Supplemental Figure 2. Effects of αGC on serum levels and myocardial gene expression of cytokines in the normal mice

(A) Serum levels of IL-10, IL-4 and IFN-γ0, 0.5, 1, 3, 6, 12 and 24 hr after αGC intraperitoneal injection into the normal mice (0.1 μg/g body weight). n=6 for each group. **(B)** Quantitative analysis of IL-10, IL-4 and IFN-γ mRNA expression in the myocardium after αGC injection. n=6 for each group. Data are expressed as means±SE. * $P<0.05$ vs. 0 hr. ND, not detected.

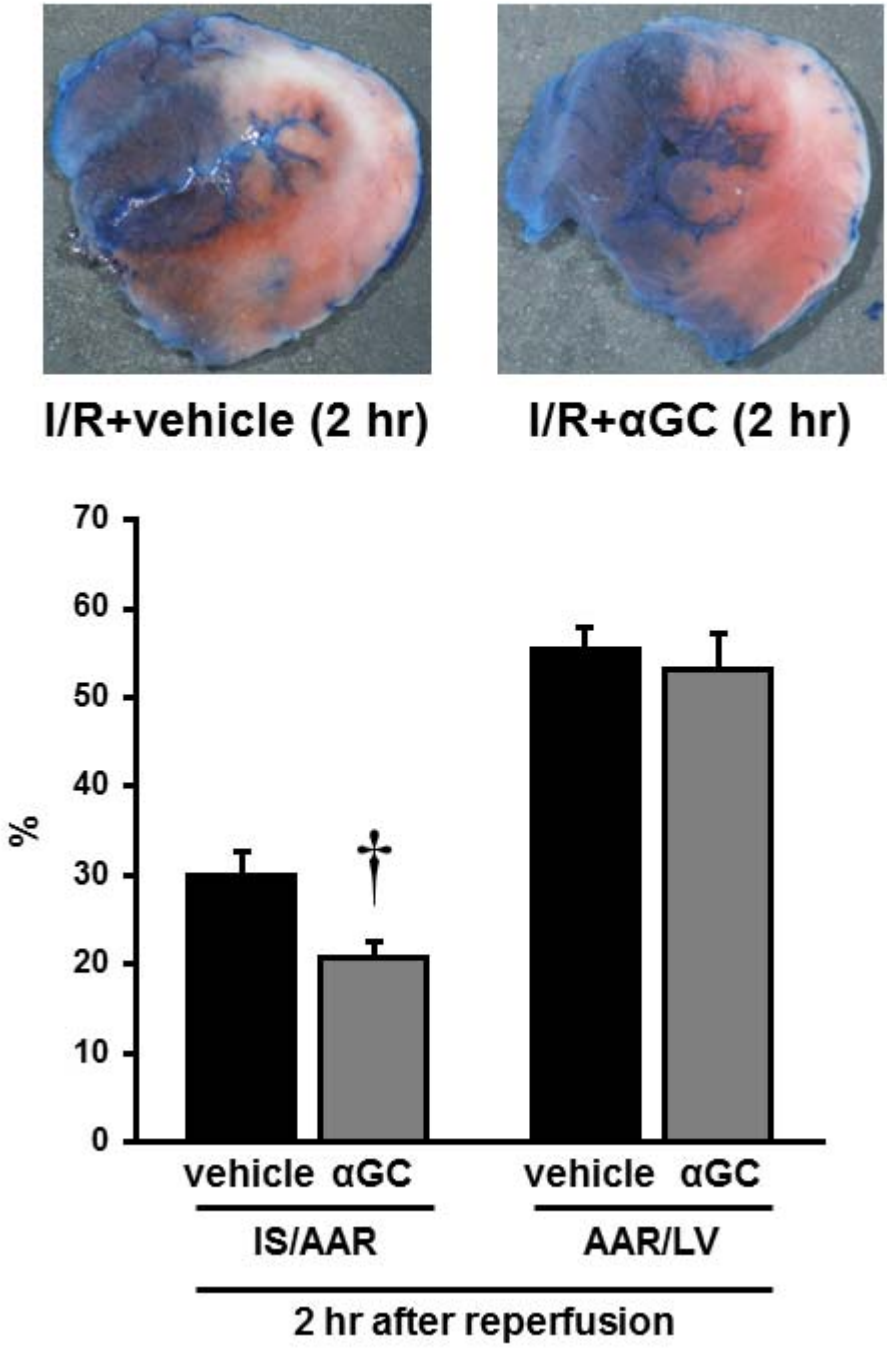

Supplemental Figure 3. Effects of αGC on myocardial I/R injury at 2 hr

Representative pictures of Evans Blue and TTC-stained LV sections 2 hr after reperfusion from I/R+vehicle and I/R+αGC (upper panels). IS/AAR and AAR/LV 2 hr after reperfusion in I/R+vehicle

(n=7) and I/R+αGC (n=8) mice (lower panel). Data are expressed as means±SE. † P<0.05 vs. I/R+vehicle.

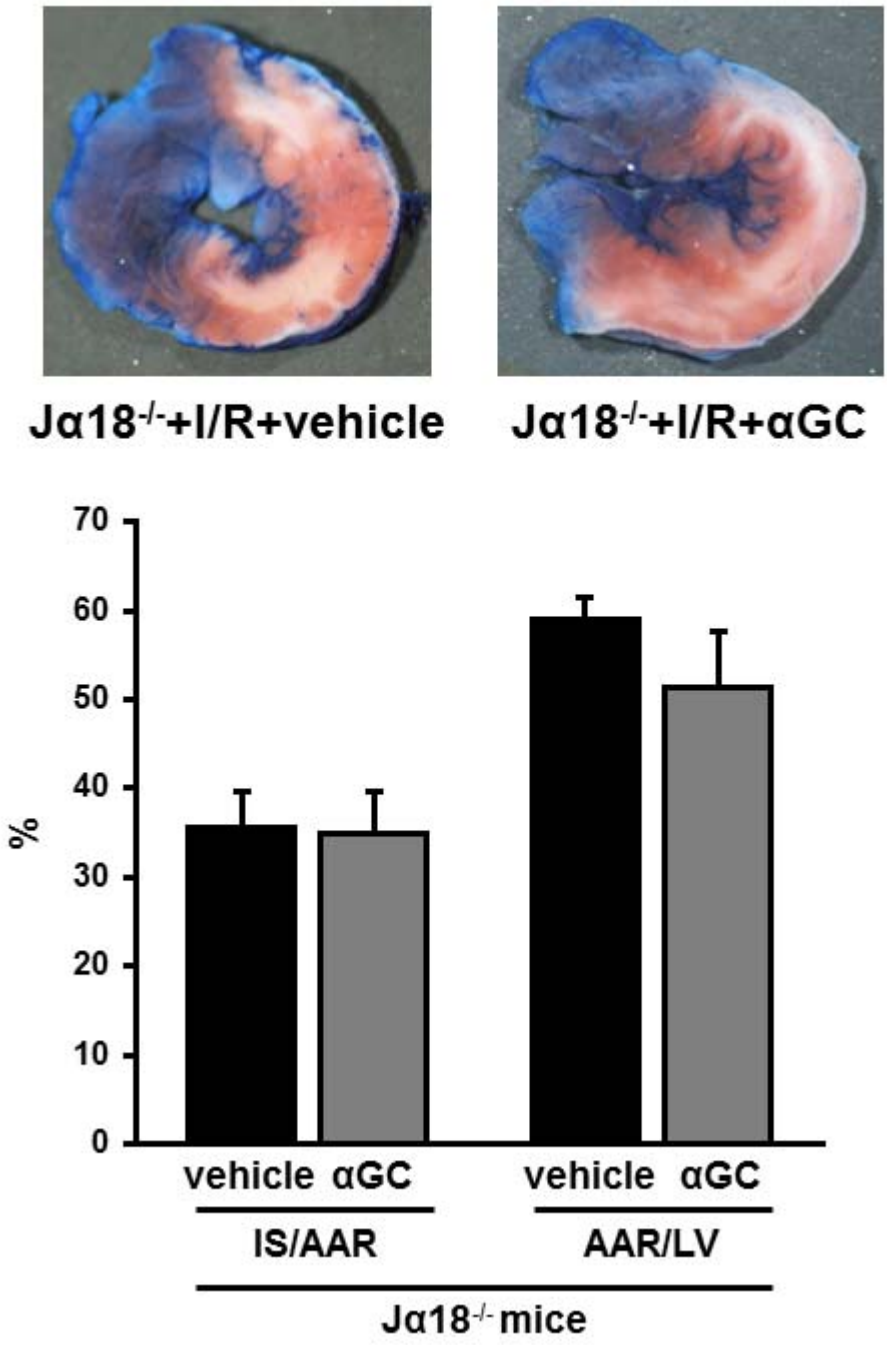

Supplemental Figure 4. Effects of αGC on myocardial I/R injury in Jα18$^{-/-}$ mice

Representative pictures of Evans Blue and TTC-stained LV sections from Jα18$^{-/-}$+I/R+vehicle and Jα18$^{-/-}$+I/R+αGC (upper panels). IS/AAR and AAR/LV 24 hr after reperfusion in Jα18$^{-/-}$+I/R+vehicle (n=5) and Jα18$^{-/-}$+I/R+αGC (n=5) mice (lower panel). Data are expressed as means±SE.

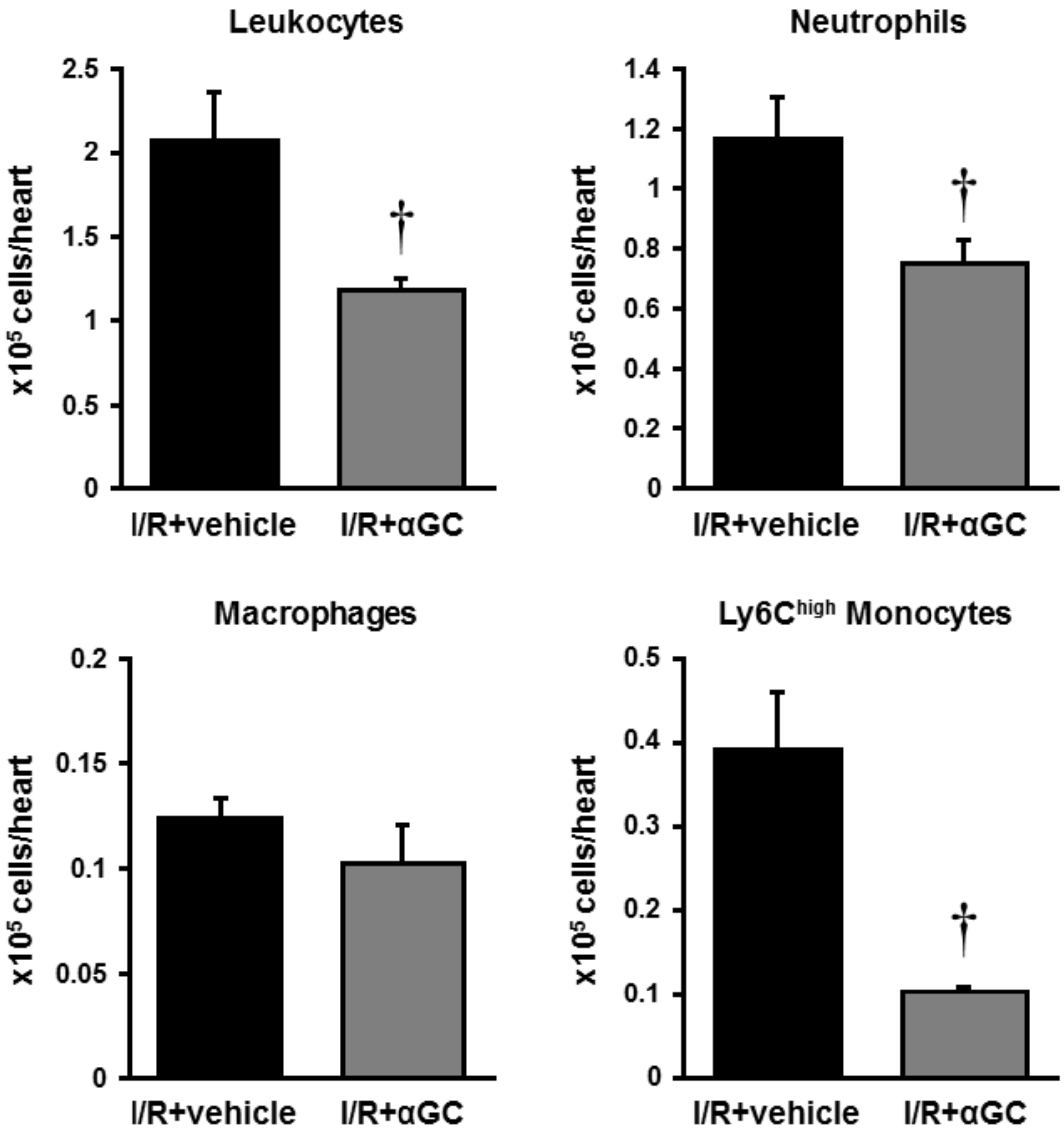

Supplemental Figure 5. Effects of αGC on the infiltrating inflammatory cells in ischemic myocardium

Summary data of flow cytometric analyses of cardiac MNCs suspensions 24 hr after reperfusion from I/R+vehicle and I/R+αGC. Cardiac MNCs from 3 different mice for each group were pooled and analyzed. N=4 for each group. Data are expressed as means±SE. † $P<0.05$ vs. I/R+vehicle.

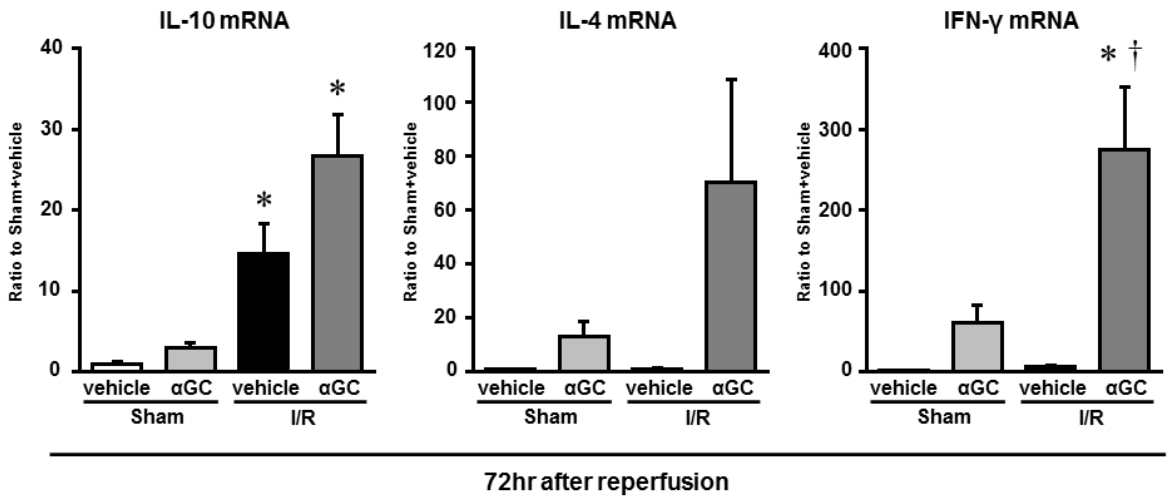

Supplemental Figure 6. Effects of αGC on myocardium gene expression of cytokines at 72 hr after reperfusion

Quantitative analysis of mRNA expression of IL-10, IL-4, and IFN-γ in ischemic myocardium 72 hr after reperfusion. n=7-8 for each group. Data are expressed as means±SE. * P<0.05 vs. Sham+vehicle. † P<0.05 vs. I/R+vehicle.

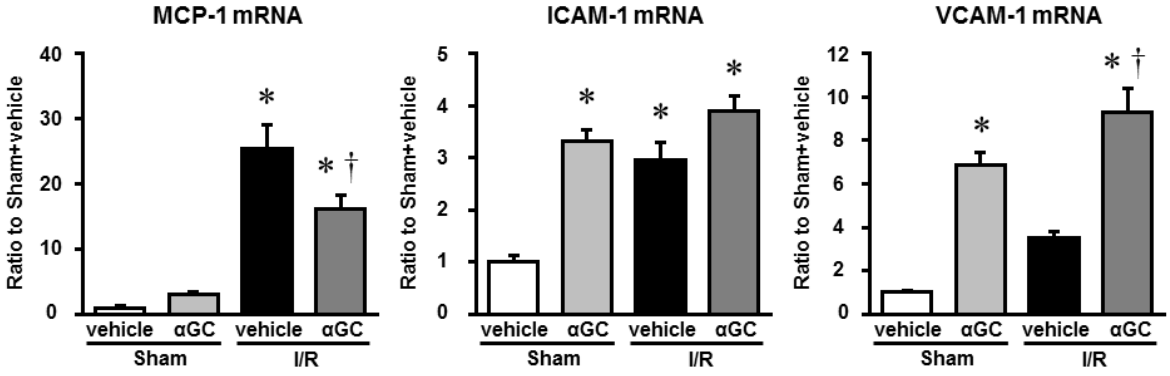

Supplemental Figure 7. Effects of αGC on myocardium gene expression of chemokines

Quantitative analysis of mRNA expression of MCP-1, ICAM-1, and VCAM-1 in ischemic myocardium 24 hr after reperfusion. n=8 for each group. Data are expressed as means±SE. * P<0.05 vs. Sham+vehicle. † P<0.05 vs. I/R+vehicle.

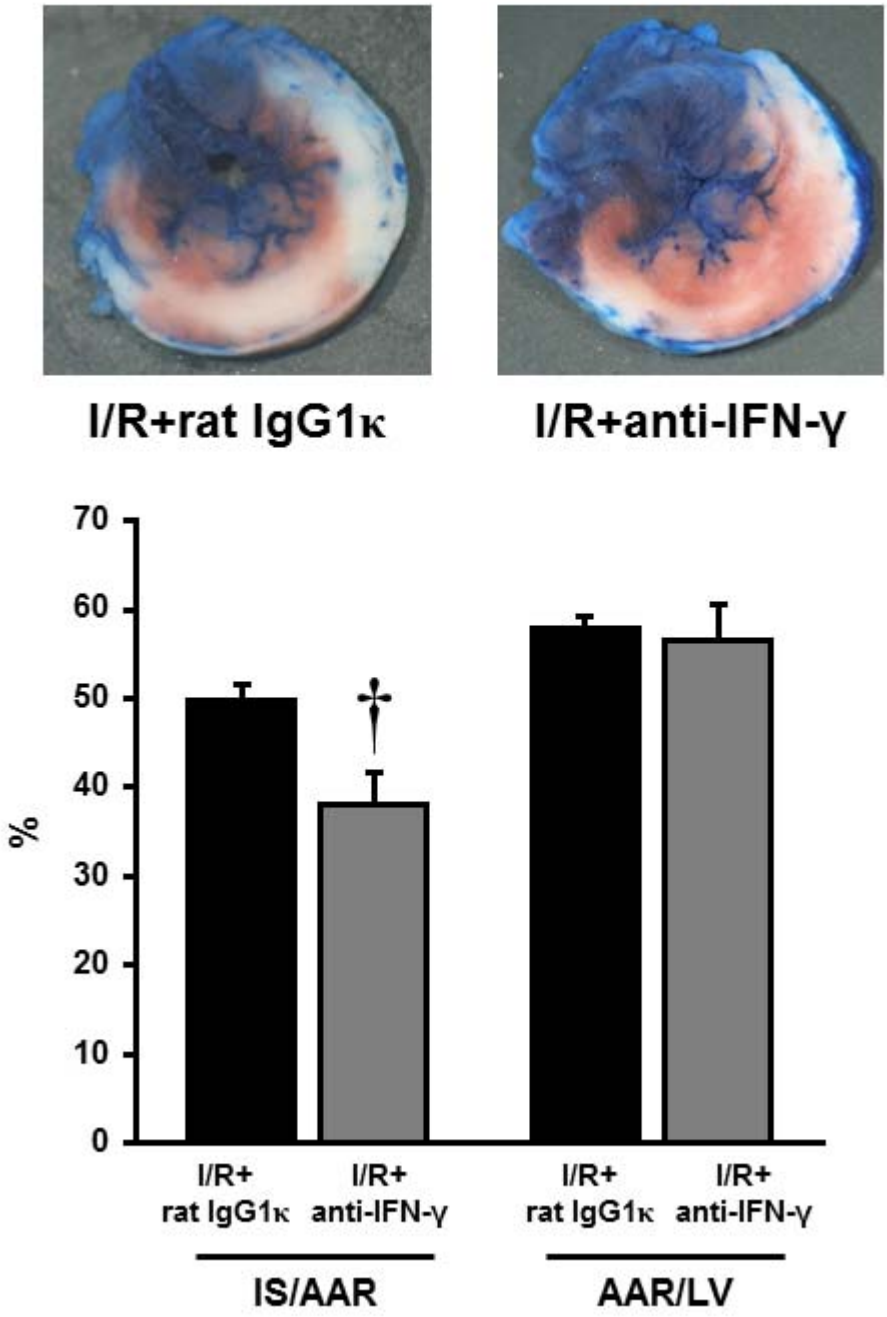

Supplemental Figure 8. Effects of anti-IFN-γ monoclonal antibody on myocardial I/R injury at 24 hr

Representative pictures of Evans Blue and TTC-stained LV sections 24 hr after reperfusion from I/R+rat IgG1κ and I/R+anti-IFN-γ mAb (upper panels). IS/AAR and AAR/LV 24 hr after reperfusion

in I/R+rat IgG1κ (n=6) and I/R+anti-IFN-γ mAb (n=6) mice (lower panel). Data are expressed as means±SE. † $P<0.05$ vs. I/R+ rat IgG1κ.

Supplemental References

[1] Nakai Y, Iwabuchi K, Fujii S, Ishimori N, Dashtsoodol N, Watano K, et al. Natural killer T cells accelerate atherogenesis in mice. Blood. 2004;104:2051-9.